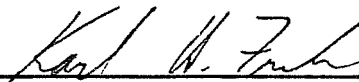
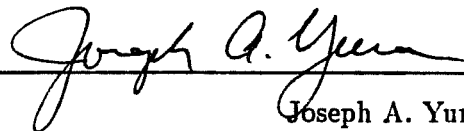


**DEVELOPMENT OF HOMOPOLAR PULSE WELDING FOR
DEEPWATER PIPELINE CONSTRUCTION**

APPROVED:



Karl H. Frank



Joseph A. Yura

To my parents Pedro and Martha, and to my brothers Pedro, Miguel, and Antonio.

**DEVELOPMENT OF HOMOPOLAR PULSE WELDING FOR
DEEPWATER PIPELINE CONSTRUCTION**

by

Francisco Javier Noyola de Garagorri, B.S.C.E

THESIS

**Presented to the Faculty of the Graduate School of
The University of Texas at Austin
in Partial Fulfillment
of the Requirements
for the Degree of
MASTER OF SCIENCE IN ENGINEERING**

THE UNIVERSITY OF TEXAS AT AUSTIN

AUGUST 1990

ACKNOWLEDGEMENTS

The author wishes to express his sincere gratitude to Dr. Karl H. Frank for his continuous guidance and friendship throughout this investigation. A very special thank you is also extended to Dr. Joseph A. Yura for all his ideas, support, and encouragement. Thanks are also extended to John Gully and Ted Aanstoos. The author also wishes to thank Dr. Jose M. Roesset for his continued support and friendship.

The author wishes to thank Kevin Farris and Mike Harville who worked as fellow graduate research assistants in this investigation. Thanks are also extended to Bob Zabcik for his supporting role as undergraduate research assistant.

The author wishes to thank the staff of the Ferguson Structural Engineering Laboratory for all the valuable help they have provided the author during this investigation. In particular, a warm thank you is extended to Wayne Fontenot for putting up with plates, pipes, charpys, and everything else.

The author wishes to thank Jose Arrellaga, David George, and Cliff Hall for their close friendship. Not only have they made life at the FSEL fun, their friendship has been a constant source of support and motivation.

Finally, the author wishes to thank his parents Pedro and Martha, and his three brothers Pedro, Miguel, and Antonio for all their love, help, and encouragement. Special thanks are extended to Antonio Noyola who has had to put up with the author while living with him for the past five years. This special thank you is accompanied with a reminder, civil engineering is better than any other engineering.

Francisco J. Noyola

May, 1990

Austin, Tx.

ABSTRACT

**DEVELOPMENT OF HOMOPOLAR PULSE WELDING FOR
DEEPWATER PIPELINE CONSTRUCTION**

by

Francisco Noyola de Garagorri, B.S.C.E

Supervising Professor: Dr. Karl H. Frank

This thesis presents a summary of work conducted at the Texas A&M-Texas Offshore Technology Research Center on the development of homopolar pulse welding for deepwater pipeline construction. This thesis presents results of structural testing conducted at the Ferguson Structural Engineering Laboratory, as well as descriptions of welder hardware. To validate the applicability of homopolar welding for pipeline construction, homopolar welds are compared and contrasted to fusion welds, to flash-butt welds, and to industrial welding requirements.

CONTENTS

	Page
Chapter 1. Introduction.	1
1.1 Deepwater Pipeline Construction.	2
1.1.1 S-Laying.	3
1.1.2 Reel Method.	5
1.1.3 J-Laying.	6
1.1.4 Resistance/Forge Welding.	7
1.2 Flash-Butt Welding.	7
1.3 Friction Welding.	9
Chapter 2. Homopolar Pulse Welding - Technical Description.	10
2.1 Homopolar Generators.	10
2.2 Electrode Configuration.	14
2.3 Hydraulic Press Configuration.	15
2.4 Monitoring of Weld Parameters.	18
2.5 Welding Process.	19
2.6 Refining Initial Weld Parameters.	21
2.7 Weld Metallurgy.	23
2.8 Advantages of Homopolar Pulse Welding.	23
Chapter 3. Testing Procedures.	24
3.1 Tension Testing.	24
3.1.1 Coupon Testing Procedure.	26

3.1.2	Full Section Testing Procedure.	27
3.2	Bend Testing.	30
3.3	Charpy V-notch Testing.	31
3.4	Base Metal Chemical Composition.	33
3.5	Ultrasonic Weld Surveys.	33
3.6	Macro-hardness Characterization.	34
3.7	Micro-hardness Characterization.	37
3.8	Weld Zone Profile Etching.	37
3.9	Microstructural Characterization.	38
3.10	Joint Surface Resistance Testing.	38
Chapter 4.	Test Results.	40
4.1	Base Metal Properties.	42
4.2	Weld Tensile Testing Results.	45
4.2.1	Tension Results. Welds made before hydraulic overhaul.	48
4.2.2	Tension Results. Welds made after hydraulic overhaul.	53
4.3	Bend Test Results.	58
4.4	Ultrasonic Testing Results.	58
4.5	Hardness Testing Results.	61
4.5.1	Macro-hardness Weld Testing Results.	61
4.5.2	Micro-hardness Weld Testing Results.	69
4.6	Charpy V-notch Testing Results.	71
4.7	Etching Results.	73
4.8	Microstructural Analysis.	75
4.9	Surface Resistance Testing.	75

4.10	Weld Temperature Measurements.	76
4.11	Effects of Post-Weld Heat Treatment.	76
4.12	Significance of Results.	78
Chapter 5. Homopolar, Flash-butt, Fusion Weld Comparison.		80
5.1	Comparison of the Weld's Thermal Processes.	80
5.1.1	Homopolar Thermal Cycle.	80
5.1.2	Flash-Butt Thermal Cycle.	87
5.1.3	Fusion Welding Thermal Cycle.	93
5.2	Comparison of Weld Turnover Rates.	94
5.3	Comparison with Industrial Standards.	94
5.4	Significance of Comparisons.	95
Chapter 6. Conclusions and Recommendations.		96
6.1	Key Results.	96
6.2	Questions for Continued Research.	96
References.		99

LIST OF TABLES

TABLE		PAGE
2.1	Criteria for parameter refinement.	22
3.1	Elements tested for during base metal characterization.	33
4.1	Summary of tests conducted to date.	41
4.2	Summary of weld parameters used.	42
4.3	Base metal tensile results - coupon testing.	43
4.4	Full section base metal tensile capacity.	44
4.5	Base metal chemical composition.	45
4.6	Summary of weld tension test results.	47
4.7	Behavior of identical welds.	52
4.8	Tensile performance of welds made after the hydraulic overhaul.	55
5.1	Weld turn over rates.	94

LIST OF FIGURES

FIGURE	PAGE
1.1 S-lay configuration.	3
1.2 S-lay production line.	4
1.3 Reel lay configuration.	5
1.4 J-lay configuration.	6
2.1 Homopolar Generator.	11
2.2 Disc and drum generator configurations.	13
2.3 Electrode casings.	14
2.4 Application of load by hydraulic press.	15
2.5 Pressure trace obtained before hydraulic modifications.	16
2.6 Pressure trace obtained after hydraulic modifications.	17
2.7 Applied pressure functions.	18
2.8 Voltage drop signaling weld completion.	21
3.1 Coupon and full section tensile specimens.	25
3.2 Stress-strain curve showing static load readings.	26
3.3 Full section tensile specimen.	28
3.4 Universal testing machine with specimen ready for testing.	29
3.5 Notch produced by weld flash.	30
3.6 Unreinforced weld specimen.	31
3.7 Charpy orientation.	32
3.8 Longitudinal ultrasonic weld survey.	35
3.9 Cross sectional ultrasonic map.	35
3.10 Location of samples used for circumferential hardness characterization.	36

3.11	Hardness specimen dimensions.	37
3.12	Etched hardness specimen.	38
3.13	Map for longitudinal hardness testing.	39
4.1	Base metal charpy v-notch data.	46
4.2	Fracture surface of weld fabricated before hydraulic modification.	49
4.3	Ultrasonic cross sectional map - weld 2.11.	50
4.4	Lack of fusion along inner wall - weld 2.29.	51
4.5	Comparison of weld pressure profiles - welds 2.26 vs. 2.29.	53
4.6	Comparison of pressure profiles made before and after hydraulic modification.	54
4.7	Specimen that passed the tensile test.	56
4.8	Weld 2.36 after being tested.	57
4.9	Tested bend specimen.	59
4.10	Comparison of ultrasonic evaluation and specimen fracture surface.	60
4.11	Lack of fusion along inner wall.	61
4.12	Band of expected hardness variation - Outer pipe wall.	62
4.13	Band of expected hardness variation - Mid- thickness.	63
4.14	Band of expected hardness variation - Inner pipe wall.	64
4.15	Location of electrode contact zone.	65
4.16	Overall homopolar hardness range.	66
4.17	Average weld hardnesses.	67
4.18	Weld line hardness profiles.	68
4.19	Location of hardness specimens. Welds 2.08 and 2.11.	69
4.20	Circumferential hardness variation.	70
4.21	Micro-hardness and macro-hardness results - weld 2.22.	71

4.22	Homopolar toughness performance.	72
4.23	Typical etch patterns.	74
4.24	Effects of post-weld heat treatment on weld hardness.	77
5.1	Interface heating during the first homopolar thermal phase.	81
5.2	Bulk heating during the second homopolar thermal phase.	82
5.3	Weld cooling during the third homopolar thermal phase.	83
5.4	Recorded parameter traces - weld 2.22.	84
5.5	Cumulative energy trace - weld 2.22.	85
5.6	Base metal micrographs. 100X and 400X magnifications.	86
5.7	Weld plane micrographs. 100X and 400X magnifications.	88
5.8	Heat affected zone micrographs. 100X and 400X magnifications.	89
5.9	Homopolar vs. flash-butt weld hardnesses.	91
5.10	Homopolar vs. flash-butt weld toughnesses.	92

CHAPTER 1

INTRODUCTION

The growing need for the development of deep sea resources has led to increased research within the area of deepwater engineering. The National Science Foundation has created a research center at Texas A&M University and at The University of Texas at Austin whose purpose is the investigation and development of new deepwater technology. Through it, investigators have attempted to touch a wide variety of areas. Research tasks have ranged from the development of new tension leg platform schemes, to the development of deep sea pipe laying technology. As part of the initial work done at the Offshore Technology Research Center, researchers at The University of Texas' Center for Electromechanics and at the Ferguson Structural Engineering Laboratory have been working on the development, characterization, and codification of homopolar pulse welding.

Homopolar pulse welding is a solid state resistance/forging process which uses the discharge current pulse of a homopolar generator to join two or more work pieces.(1). This process is very similar to flash-butt welding. Unlike flash-butt welds, homopolar welds are completed in seconds. Its capacity for fast one station welding makes homopolar welding an attractive alternative for deep sea pipe construction.

The development of homopolar pulse welding coincides with the industry's shift from S-laying to J-laying. Traditional laying techniques can no longer be used in deepwater projects. Both structural and mechanical problems limit the applicability of such laying schemes to work done in water depths ranging up to 1500 ft. J- laying offers an attractive solution for deepwater pipeline construction. To be incorporated, however, a fully automatic, reliable, and fast welding system must first be developed. Both flash-butt and homopolar pulse welding are strong contenders for such a task.

This thesis presents a discussion on the initial work done at the Ferguson Structural Engineering Laboratory and at the Center for Electromechanics on homopolar welding for pipeline construction. Eighteen 3.5" x 0.42" homopolar welds were fabricated and tested. From these welds, tensile, hardness, toughness, thermal, and metallurgical homopolar characterizations were developed.

Before presenting any discussion on homopolar welding, however, a brief discussion on pipeline welding trends, and in particular on flash-butt welding, is given. Flash-butt welding is a resistance/forging welding process that is well suited for deepwater pipeline construction. Because of this, homopolar weld and flash-butt weld properties are then compared and contrasted to establish the applicability of homopolar pulse welding as a viable pipeline construction system. This discussion is presented in chapter five.

1.1 DEEPWATER PIPELINE CONSTRUCTION.

Current trends in today's oil market have renewed an interest for the exploitation of deep offshore oil fields. High energy demands have created a need for deep sea hydrocarbons. Because of this, new facilities are being planned for placement in ocean depths ranging between 1000 and 6000 ft of water. Before such systems can be realized, many questions concerning deepwater construction must be answered.

The fabrication and laying of pipeline in deepwater is one area of offshore construction which has received much attention. Changes in all phases of pipeline fabrication are needed if these facilities are to be placed in the deep sea. Improvements in materials, in laying techniques, in welding equipment, and in overall quality assurance must be achieved. Added to these, more stringent construction standards, similar to those found within the BS 4515-84 "Process of Welding of Steel Pipelines on Land and Offshore" and the Det Norske Veritas 81 (DnV-81) "Rules for Submarine Pipeline Systems", need to be developed.(2).

Given today's materials, the controlling factor affecting the feasibility of deep sea pipeline construction seems to be the development of a new laying scheme. To date, most offshore pipelines have been fabricated using either a horizontal laying arrangement (S-laying) or a reel system.

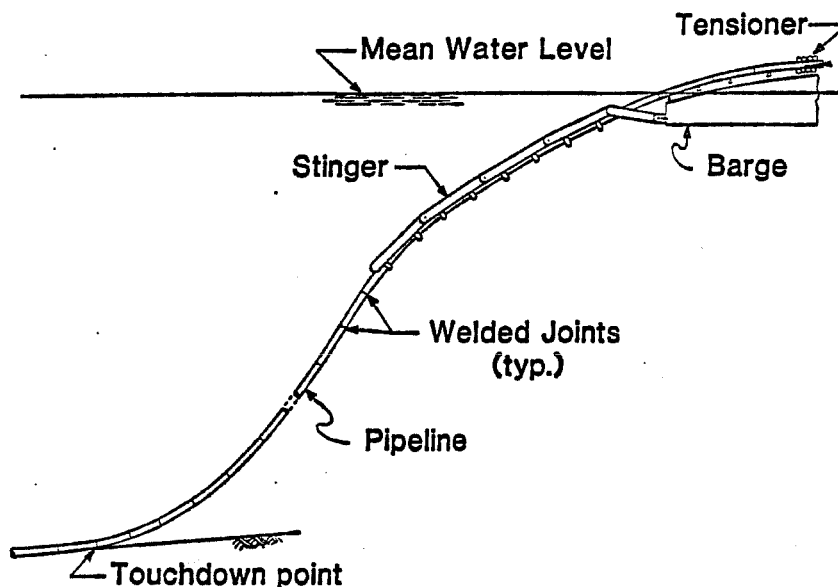


Figure 1.1 S-lay configuration.(4).

1.1.1 S-LAYING.

Pipelines 16 to 36 inch in diameter have been primarily placed using the S-lay configuration.(3). As shown in Figure 1.1, this scheme gets its name from the characteristic shape of the line during laying. Due to the severity of its bending stresses, S-laying cannot be used in water depths exceeding 1000 ft without running the risk of pipe buckling.

In the horizontal operation mode, welding on a lay barge is broken up into a series of tasks; each task conducted by specialized work stations along a main production line. A schematic of this is shown in Figure 1.2. Fabrication of a joint starts by positioning a new pipe segment at the front of the production line. Weld production begins at this location with the complete deposition of a root pass. The barge is then advanced to accommodate a new line segment. Additional passes are deposited by each work station along the barge. Wrapping of the joint, post weld

heat treatment, weld inspection, and flash removal are conducted as the joint reaches the last work station. The finished joint is then rolled onto the barge's stinger, and lowered into the ocean. Note, all preweld joint preparations are completed in satellite stations away from the main production line.

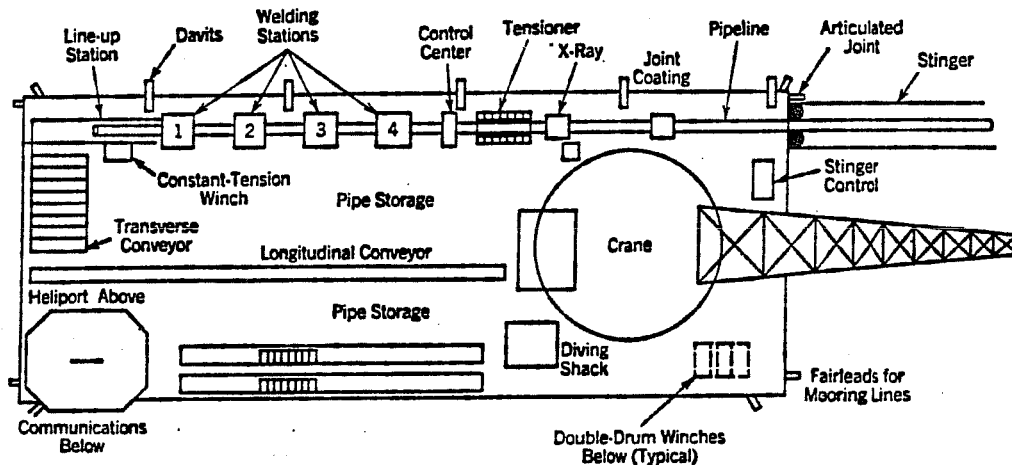


Figure 1.2 Horizontal production line arrangement.(5).

Tensioners between weld stations hold the line in place during line construction. Since the welded joint is completed in several welding stations, care must be taken to ensure that each stage of the partially completed weld has enough resistance to withstand the overall stress level at that location along the line. Tensioners provide the support required to prevent joint distress.

In addition to joint support, tensioners impart a tensile load on the line to reduce the risk of pipe buckling. The severity of S-lay bending stresses is reduced with the introduction of an axial tensile stress. The magnitude of the required tensile load is a function of water depth, pipe diameter, pipe wall thickness, pipe yield strength, and stinger configuration.(2). Note, deeper water requires a higher tensile stress. There are, however, practical, structural, and mechanical limitations that set an upper bound to the level of load that can be applied. "Present day pipe lay barges are limited to a maximum working depth of 1500 ft. In addition to

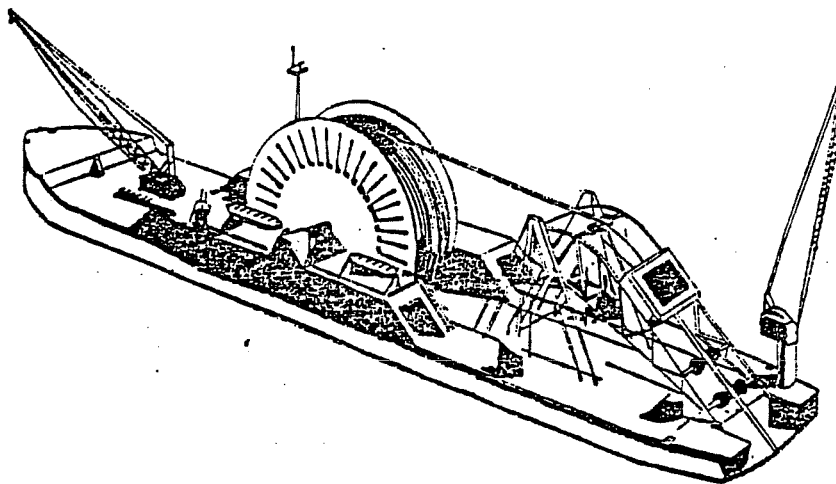


Figure 1.3 Reel laying configuration.(5).

this, 36 inch diameter pipe cannot be laid using conventional means without fear of weight-coat damage, buckling, or simple over stressing.”(6).

More stringent limits on the size and location of allowable weld repairs are required as work moves into deeper waters. Repairs, which in the past were allowed after the last tensioner, may no longer be allowed. These would have commonly included the repair of small root defects.(2). Therefore, weld evaluation tasks will have to be conducted closer to the weld pass stations where high weld temperatures may still be present. Having the barge back up in order to repair, or replace a joint, is highly undesirable with the increased risk of pipe damage at larger depths.

1.1.2 REEL METHOD.

Smaller diameter lines have generally been laid using the reel method. A schematic of this arrangement is shown in Figure 1.3. As currently done, the reel method produces the same characteristic “S” shape line geometry as S-laying. Because of the high bending stresses associated with this geometry, reel laying runs the same risk of inducing pipe buckling in deepwater as S-laying.

1.1.3 J-LAYING.

To eliminate structural limitations, the application of a new pipe laying scheme, shown in Figure 1.4, is currently being considered by the offshore industry. Vertical pipe laying, J-laying, provides an attractive conceptual alternative for deep sea work. Unlike S-laying, J-laying does not produce severe construction stresses. Therefore, the applicability of J-laying is independent of water depth.

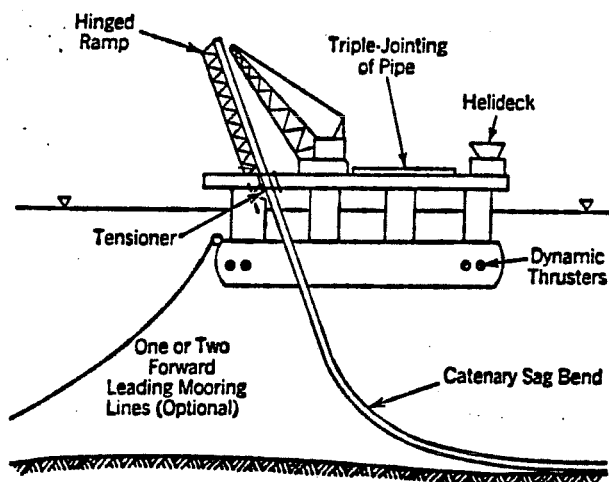


Figure 1.4 J-lay configuration.(5).

Any welding system adapted for J-laying must meet several requirements. Unlike S-laying, space is a factor in the vertical laying mode. The number of allowable work stations is limited by the height of the barge deck above sea level, and by the height of the pipe support derrick.(6). Therefore, any welding system that is to be used in J-laying must be capable of completing a weld in very few stations. The system must also be capable of meeting a strict quality assurance criteria soon after finishing a joint. Having less welding stations shortens the time before new line segments reach the ocean. Finally, the welding system should be fast. High laying rates are required with current lay barge operation costs reaching \$400,000 a day.(7).

The need for J-laying has made the development of new welding technology a priority. Efforts aimed in this area have resulted in the development of several alternative automatic welding systems. Among these are flash-butt welding, explosion welding, friction welding, automatic gas metal arc welding (GMAW), and now homopolar pulsed welding.

1.1.4 RESISTANCE/FORGE WELDING.

Due to the characteristics of resistance/forge systems, flash-butt welding and homopolar pulsed welding seem to be the best suited alternatives for incorporation into a J-lay configuration. These processes do not require the use of either filler or flux material. This greatly simplifies the metallurgical properties of the joint. Fusion problems associated with other automatic processes are not seen in a resistance/forge arrangement. Lack of sidewall and interrune fusion has led to serious questions concerning the adequacy of GMAW.(8). In addition, resistance welding offers higher production rates than most other automatic processes. Finally, and most importantly, only one welding station is required by resistance/forge welding systems.

Since similarities exist between flash-butt and homopolar pulsed welding, a description of flash-butt welding will help in developing an understanding of homopolar welding. In addition, an assessment of the applicability of homopolar pulsed welding can be made by comparing the properties of homopolar welds to those of flash-butt welds.

1.2 FLASH-BUTT WELDING.

Flash-butt welding is a fully automated resistance/forging welding process. Joint pieces are heated through joint surface current resistance, and forged together by an applied upset pressure. Clamping electrodes supply the necessary electric current and upset load. All power is obtained from a DC diesel generator. Key weld parameters are monitored through strip chart recorders. Flash-butt welding has been certified by both the API and AGA as an allowable joining process for lines having diameters ranging between 16 and 36 inches.

The following sequence of steps is used in making a flash-butt weld. Electrical contact shoes are first securely clamped to the two pipes that are to be welded. Then, while low voltage current is applied, the pieces are slowly moved together. Electrical contact is made as asperities within the joint interface touch. As this occurs, resistance heating and local current densities produce flashing. Flashing is allowed to continue for a predetermined duration of time based on the size of the joint. Once this time elapses, and enough heat is generated, an axial forging load is then applied to the pipes. Inclusions are expelled from the joint as pipe upset occurs. Note, a roughened end surface must be used to produce sufficient interface heating. As mentioned above, flashing is a function of surface resistance. Using smooth surfaces may result in insufficient heat generation.

Flash-butt welding is a high heat input, slow heating, slow cooling process. Because of this, grain growth in the austenitic range occurs. Post weld heat treatment must be applied to eliminate this problem.

All excess weld flash must also be removed. API standards limit the amount of reinforcement on a joint to 1/16 in. for the interior pipe wall and 1/8 in for the exterior wall.

Flash-butt welding has been shown to have great a potential as a high productivity pipe joining process. Seven minute turnover rates have been achieved while welding 36" x 1" pipe.(7). This is faster than most automatic or semiautomatic welding systems.(7). Some studies have shown that using flash-butt welding as opposed to fully automatic GMAW leads to a 25in weld cycle time.(3). Such a reduction is significant in terms of lay barge economics. Flash-butt systems require a small number of operators since it is fully automated. Only one fifth the personnel is required when compared to other weld procedures and the level of required operator specialization is low.(3). Fully completed flash butt welds can be obtained in three stations, hence meeting J-lay space limitations. Finally, an adaptive control system helps guarantee consistent weld quality. Key parameters are monitored by strip chart recorders so initial weld evaluations can be made instantly.

1.3 FRICTION WELDING.

Friction welding is another forge welding process suggested for the welding of pipe. Unlike flash-butt and homopolar welding, friction welding does not rely on resistance heating. Welding is achieved through friction heating.

As its name implies, friction welding uses workpiece friction as a heat source. In this process, one pipe section is held stationary and fixed, while the other pipe section is rotated about its axis. Having achieved a desired rotational speed, the rotating pipe is brought next to the stationary pipe. Contact is made using a preset friction pressure.(9). Heat at the weld surface is quickly generated. The rotating section is then allowed to upset for a preset burn off distance.(9). As this occurs, excess material is expelled from the weld zone. Having undergone the desired burn off distance, the rotating pipe is stopped and an upset forging load is applied. This completes the friction weld. Twelve minute turnover rates may be obtained while welding twelve inch pipe.(9).

Both post weld heat treatment and flash removal are conducted after finishing the weld. A by product of friction welding is a severe flash which must be removed.

Friction welding has not acquired wide spread popularity in the welding of carbon steels due to its high capital equipment cost. Friction welding is seen as a useful process for the welding of more exotic materials and for the welding of stainless steel. Only when welding these materials does friction welding show cost effectiveness.(9). Therefore, it is unlikely that friction welding will receive much attention for utilization in J-laying.

CHAPTER 2

HOMOPOLAR PULSE WELDING- TECHNICAL DESCRIPTION

Homopolar pulse welding is a solid state resistance/forge welding process. Like flash-butt welds, homopolar pulse welds rely on interface surface resistance for heat generation. Added to this, an applied upset load is used to forge the joint. Unlike flash-butt welding, homopolar welding uses the discharge current pulse of a homopolar pulse generator to provide the weld energy.

2.1 HOMOPOLAR GENERATORS

The main difference between the homopolar welding and the flash-butt welding process lies in the energy source. While flash- butt welding relies on a DC diesel generator, homopolar welding uses a homopolar generator power the weld.

As described in the literature published by The University of Texas Center for Electromechanics:

The homopolar pulse generator is an electric machine which converts stored rotational kinetic energy into electrical energy using the Faraday effect. It is a low voltage, high current device that is most advantageously operated in the pulsed mode. Because of this, homopolar pulse generators are an excellent power source for applications that require short time, high power energy pulses. Having a pulsed mode operation allows the generator to accept and store energy continuously from a low power source, and then deliver this energy to a load in the form of a controlled shape, high power pulse.

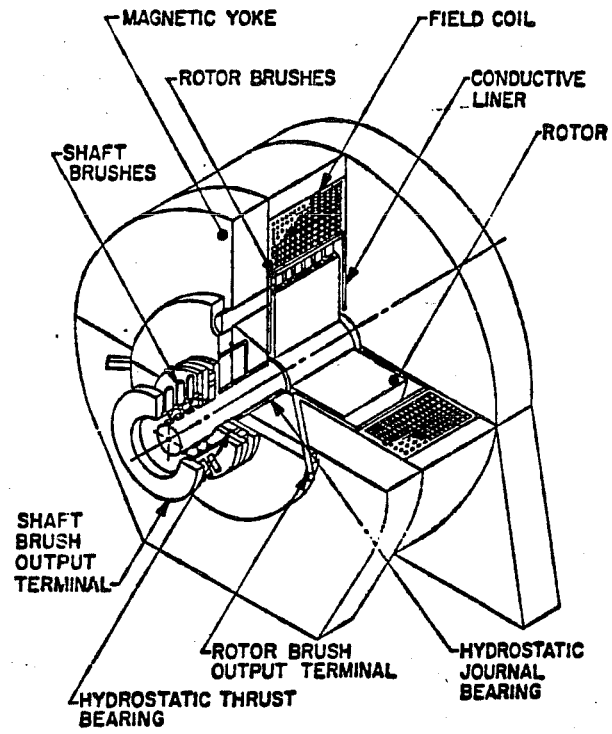


Figure 2.1 Homopolar generator.(10).

As shown in Figure 2.1, homopolar generators consist of a cylindrical metal rotor spinning in a magnetic field. The rotor is supported at its ends by stub shafts mounted in low friction, high stiffness bearings. These bearings are in turn supported by bearing housings mounted within the machine's yoke. The yoke serves as the generator's main structural element and, in most machines, as the return path for the applied magnetic field. The magnetic field is produced by one or more simple solenoids mounted inside the yoke. This field provides the generator with the excitation needed to produce a current pulse discharge. Copper graphite composite electrical brushes, bus bars, and conductors, are used to transfer current into and out of the rotor.(1).

Because of low internal impedance, homopolar pulse generators are capable of efficiently converting stored mechanical energy into a high current, high power, electric pulse. These machines are capable of storing 5.0 KJ/kg and then converting it to megampere peak current pulses at average powers of 50 KW/kg. These characteristics make inertial iron core homopolar pulse generators efficient power supplies for very rapid heating of resistive loads.(11).

Note, both disc and drum generator configurations exist. These are shown in Figure 2.2. Disc machines use an applied axial magnetic field in the rotor and a radial current flow. Drum machines use a radial magnetic field and an axial current flow. Both types are usually powered by a hydraulic motor.(12).

A ten megajoule disc generator was used to produce all the welds in this research project. The generator was spun at 3000 rpm for most of the welds. A hydraulic motor was used to bring the generator up to proper welding speed

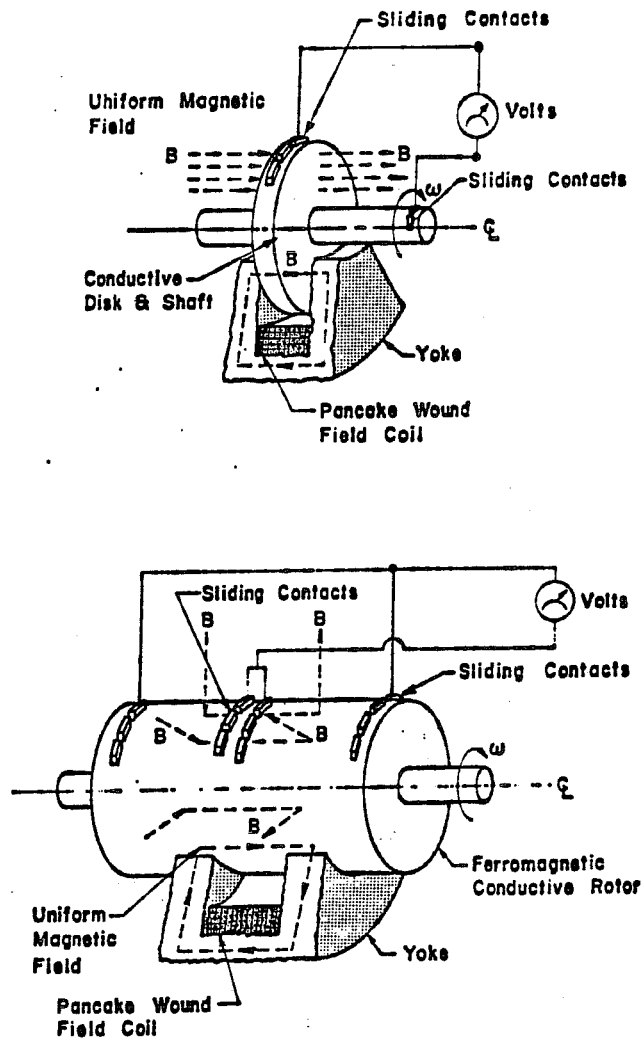


Figure 2.2 Disc and drum generator configurations.(12).

2.2 ELECTRODE CONFIGURATION.

Copper composite electrodes deliver the current pulse to the pipes. The electrode casings shown in Figure 2.3 were used in the production of welds discussed within this thesis. Each casing has 12 current conducting fingers that deliver energy to the weld. Using this finger arrangement helps assure a circumferentially homogenous current distribution.

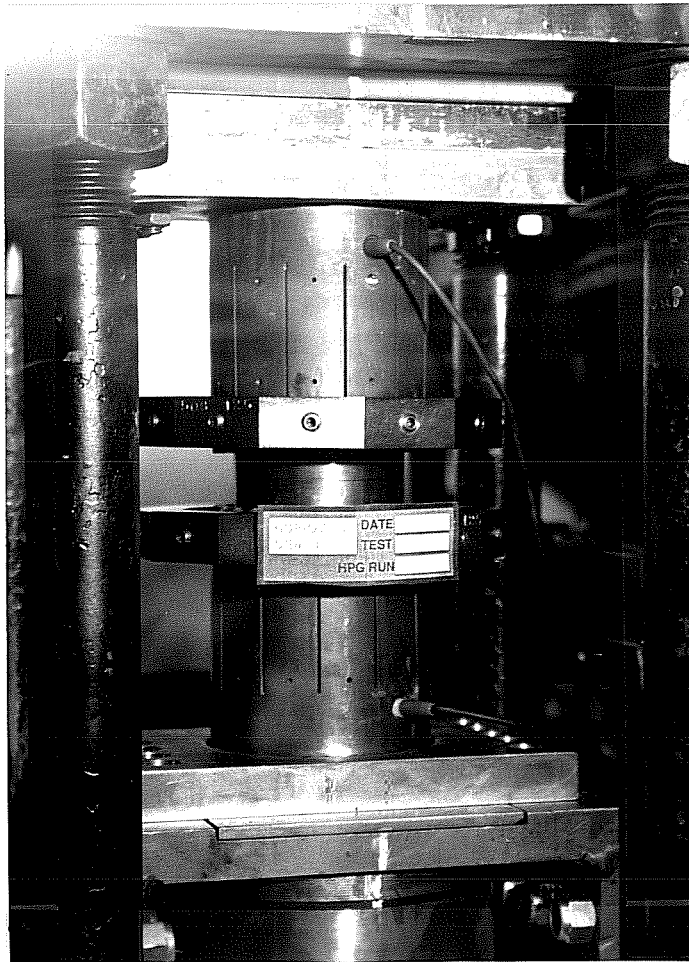


Figure 2.3 Electrode casings.

2.3 HYDRAULIC PRESS CONFIGURATION.

Both initial and upset loads are applied externally through a hydraulic press. As shown in Figure 2.4, load is applied axially to the pieces being welded.

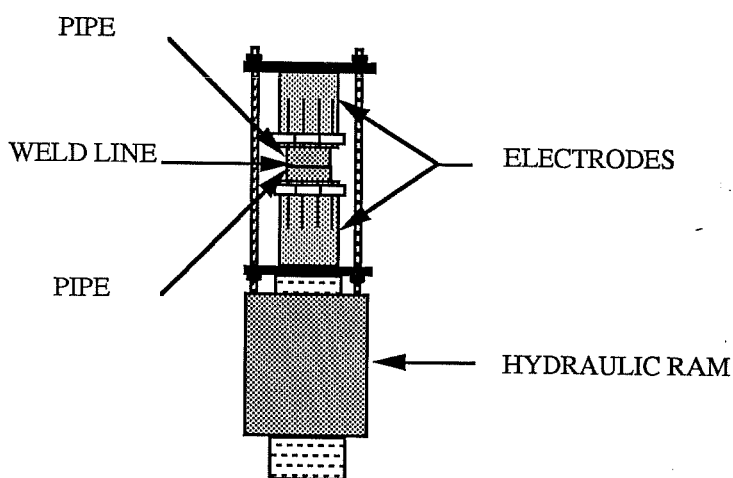


Figure 2.4 Application of load by hydraulic press.

The system's hydraulic configuration has undergone significant changes since starting the homopolar pulsed welding research program. Initially an open loop hydraulic system was used to control the application of loads during welding. This configuration proved to be inadequate due to lack of hydraulic load control.

Figure 2.5 shows a pressure versus time plot for a weld made before the hydraulic overhaul. A gradual increase in initial pressure caused by pipe thermal expansion is seen before the application of the upset forging load. Note, pressure

drifting began to occur at 0.6 secs. As discussed in chapter four, it is believed that such increases in pressure lead to reduced surface resistance, therefore resulting in low interface heat generation.

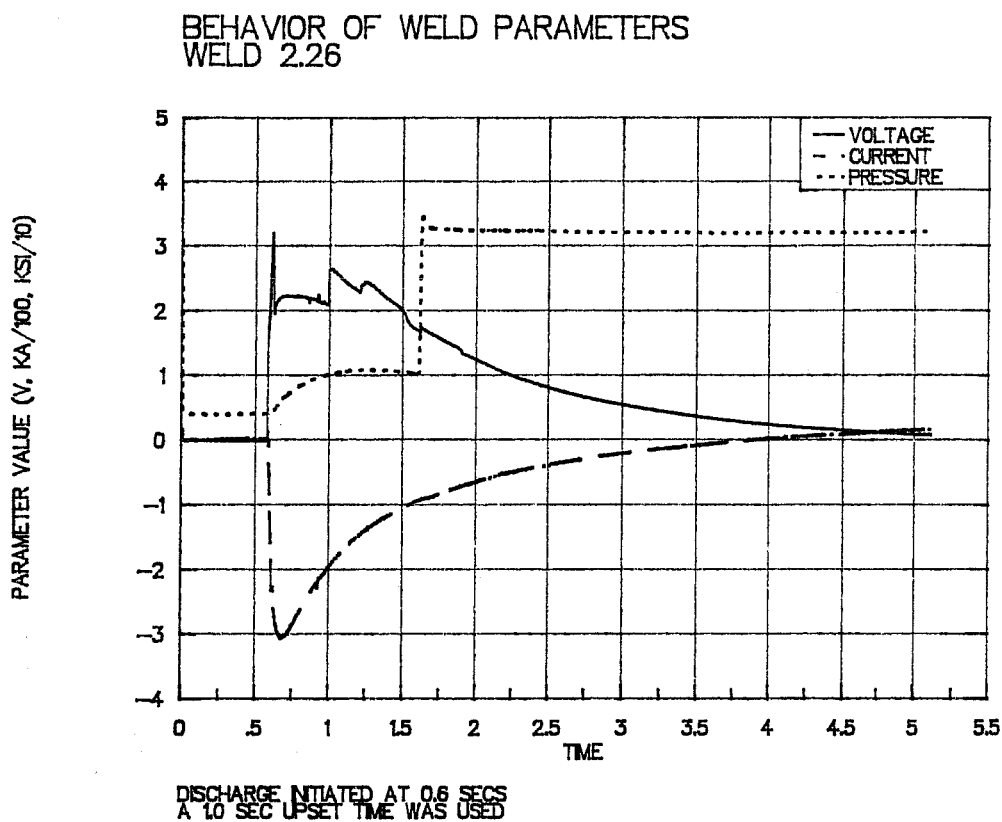


Figure 2.5 Pressure trace obtained before hydraulic modification.

In an effort to obtain better pressure control, a closed loop servo-controlled hydraulic system was designed and installed. A Moog servo-valve is used in conjunction with a Pegasus servo-controller. In addition, an Exact function generator was incorporated in order to have the flexibility of changing the shape of the forging

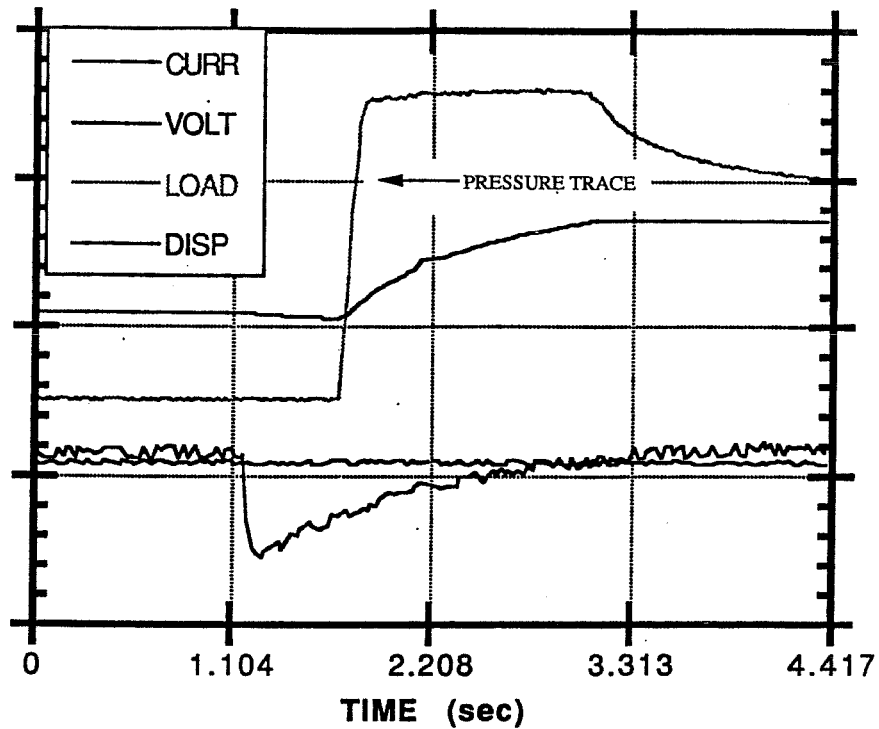


Figure 2.6 Pressure trace obtained after hydraulic modification.

pulse. As shown in figure 2.6, initial pressure drifting was eliminated through the use of this new hydraulic system.

A schematic of a square wave and a ramped pulse is shown in Figure 2.7. Using a ramping function, as opposed to a square wave, may result in longer interface heating. So far, only square forging pulses have been used to produce welds.

An accumulator and a line tamer were also installed to achieve better hydraulic control. A five gallon accumulator was required to provide enough fluid capacity for the forging pulse. A line tamer was used to provide filtering, additional accumulation, and hydraulic pressure switching.

APPLIED PRESSURE PROFILES

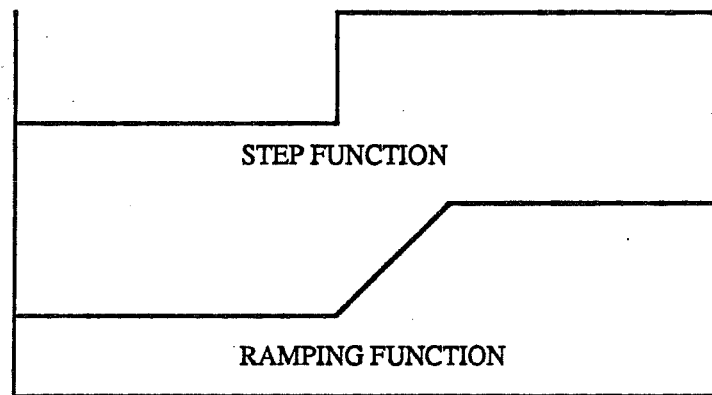


Figure 2.7 Pressure functions.

2.4 MONITORING OF WELD PARAMETERS.

Key weld parameters are recorded by a separate data acquisition system. Traces of the generator's RPM's, voltage, current, load, and displacement can be obtained after welding. Two set of traces were shown in Figures 2.5 and 2.6. The generator's RPM's, the voltage potential across the workpieces, and the weld current are monitored directly through the machine's control system. Loads are monitored through a 200 kip Interface load cell. Displacements are recorded through a 2 inch linear potentiometer. Outputs for all traces are generated as both digital output files and strip chart recordings. Quality assurance flags may be found through the use of this data acquisition system. Monitoring these flags may allow rapid weld evaluations after finishing a joint. Rapid weld evaluations are necessary if homopolar welding is to be incorporated into a J-lay fabrication arrangement.

2.5 WELDING PROCESS

As described before, homopolar pulsed welding is a resistance/forge process in which two or more contacting workpieces conduct the discharge current pulse from a homopolar pulse generator. Resistance heating occurs along the joint surface due to the constriction of current at small surface asperities. Heating is allowed to continue for a predetermined time period. After sufficient heat is generated, an upset load is applied to forge the workpieces together.

The process begins with the selection of proper welding parameters. Rotor speed, field current, initial interface pressure, upset pressure, and time of upset, are the weld parameters that are directly controlled by the system's operator. Proper parameters must be preprogrammed into the homopolar's control system before welding a new material or cross section.

The following criteria are used in choosing initial weld parameters. First, desired rotor speed is set according to weld size. Second, a value for open circuit voltage is chosen. Approximately fifteen volts are needed to produce adequate pulses for welding steel.(11). Open circuit voltages are produced and controlled by the solenoid's magnetic field, therefore the amount of current supplied to the solenoid is controlled by the desired value for open circuit voltage. Third, an initial contact pressure is selected. In addition to surface preparation, surface resistance is a function of the square root of the apparent contact pressure.(11). Therefore, the amount of interface heat generation is a function of initial contact pressure and surface roughness. Fourth, a value for upset pressure is set. Forging pressures are selected according to material yield strength at welding temperature. Finally, time of upset is selected to occur at, or near to, peak interface temperature. So far, the initial selection of upset times has been based on past experience due to lack of real time control.

After selecting the desired weld parameters, all pipe surface preparations are then carried out. A roughened end surface, such as that produced a band saw, is needed to produce sufficient interface resistance. Smooth surfaces may result in insufficient heat generation. In addition, the pipe's electrode contact zone must be cleaned before welding. Local arcing at this location should be avoided. Sand blasting and the use of cleaners, such as acetone, provide good contact surfaces.

After completing all surface preparations, the pipes are then secured within the electrode casings. Care is taken to ensure that contact is made all along the circumference of the pipe. If gaps exist between the pipes and electrodes, thin conductive shims are used to provide full electrical contact.

After fixing the pipes within the electrode casings, the pipes are then placed within the welding fixture. Care is taken to ensure the best possible pipe alignment. Initial preloading is then applied to the aligned pipes. As was shown in Figure 2.7, the level of initial contact pressure is maintained until the application of the weld's forging load.

The homopolar generator is then brought up to speed using a hydraulic motor. Since rotational kinetic energy is converted to electrical energy, welding energy is a direct function of rotor speed. Reaching the desired rotor speed level takes only a few minutes.

Current is supplied to the generator's solenoid after reaching speed. The magnetic field induced by this current provides the excitation needed to produce discharge. Having charged the system, current collecting brushes are actuated. A closing switch is then used to initiate discharge. "During discharge, all or part of the kinetic energy stored in the rotor is electromagnetically converted into electrical energy."(11). The generator's hydraulic motor is then turned off, and the rotor allowed to stop.

Although steel has some resistivity, heat generation is concentrated at the interface due to the constriction of current within the small areas of real contact. Pressure is maintained at preload level in order to maximize heat generation at the interface. If pressure is increased too fast, electrical surface resistance is lost before enough heat is generated.

The pipes are forged at peak interface temperature. A simple timer is used to trigger the function generator, which in turn, triggers a load step. Load is increased beyond the material's yield capacity at that temperature, and the pipes upset. The original surfaces coalesce due to atomic diffusion, melting, or a combination of both processes. The physics of this joining mechanism are still not well

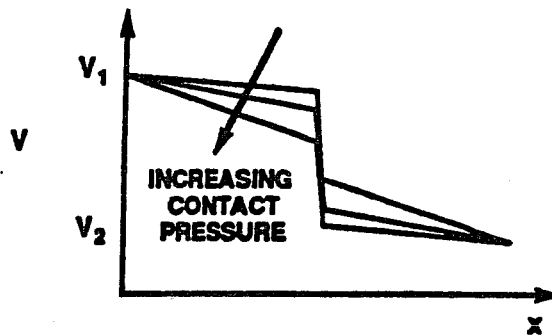


Figure 2.8 Voltage drop signaling weld completion.(11).

understood. As shown in Figure 2.8, weld completion is indicated by a sudden decrease in weld voltage. This drop in voltage is caused by the elimination of interface resistance.

Heating and cooling rates may be controlled by varying the excitation current to the homopolar pulse generator. There exists a possibility that pre and post weld heat treatments may be applied by using a shaped current pulse. This point will be studied as a part of the continued research work on homopolar pulsed welding.

2.6 REFINING INITIAL WELD PARAMETERS.

The evaluation of weld parameters to date has been empirical. Therefore, refinements on initial weld parameters were made through careful evaluation of test welds. Table 2.1 shows the criteria used in refining each parameter. As a part of the on going research program, parametric studies will be made to obtain relationships that will yield good estimates for weld variables. Development of parametric equations will minimize the number of required iterations before optimum welding values are obtained.

In addition to the operator controlled weld parameters, the effects of other variables on weld quality must be considered. These include current through the interface, voltage across interface, magnetic field inside the pipe, and upset displacement. Unlike the controllable parameters, the relative importance of these variables is not known. As a part of the continued research program, their effects will be studied.

TABLE 2.1 PARAMETER REFINEMENT CRITERIA.

OBSERVED WELD CHARACTERISTIC	POSSIBLE CAUSES	ALTERNATIVE SOLUTION
Cold Weld (No heat is developed at the interface)	Energy too low. Current too low. Initial Resistance too low.	Increase: Generator Speed. Open Circuit Voltage. (Solenoid Current) Surface Resistance. Decrease: Initial loading.
Bulk Heating (Heating away from interface, without obtaining a weld)	Initial Resistance too low. Application of upset was too early.	Increase: Upset Time. Decrease: Initial Loading.
Blowout (Welds produced with too much flashing)	Initial Resistance too high. Application of upset was too late.	Increase: Initial Loading. Decrease: Upset Time.
Hot Weld (Welds produced with too much bulk heating.)	Energy too high. Current too high.	Decrease: Generator Speed. Open Circuit Voltage.

Table 2.1 Criteria for parameter refinement.(11).

2.7 WELD METALLURGY.

Questions concerning the metallurgical process produced by homopolar welding exist. Although a better understanding has been established through research completed to date, a complete microstructural analysis is being planned for the near future.

2.8 ADVANTAGES OF HOMOPOLAR PULSE WELDING.

Like flash-butt welding, homopolar pulse welding offers many advantages that make it an attractive alternative for deepwater pipe laying. Homopolar welding has a high weld turn over rate due to the pulsed mode of operation. The system is fully automated. No flux or filler material is required. Welds are completed in very few stations. Finally, homopolar welding has shown to have the capacity of joining dissimilar materials, and of joining exotic metals.

In addition to an incomplete understanding of the welding process, one of the main disadvantages associated with homopolar welding is capital cost. At the present time equipment costs may reach as much as a million dollars, however investment in this technology should be justified by increased laying rates.

CHAPTER 3 TESTING PROCEDURES

Testing of both the base metal and homopolar welds has been performed. This chapter presents the procedures used during this testing.

A comprehensive analysis of base metal properties was performed at the beginning of the research program. Lone Star Steel donated 3.5" x 0.430" line pipe, no specific grade, for use in this investigation. Base metal properties were characterized according to tensile capacity, material toughness, and chemical composition. All results were then compared to the mill report.

Selection of base metal samples was done in a random manner to achieve a fair representation of the pipes' material properties. Samples were taken from a general stock pile without any particular preference with respect to pipe section or location along the pipe section. Of these samples, three sections were designated for tensile testing, and three sections were designated for charpy v- notch impact testing. Eight tensile coupons, one full section tensile specimen, and twenty four charpy specimens were fabricated from this material. Samples for chemical analysis were obtained from the grips of tested tensile coupons.

Homopolar welds were subjected to a series of weld evaluation tasks. These tasks included: tension testing using standard ASTM A-370 strap coupons, tension testing using full section specimens, ultrasonic testing, Rockwell "B" macro-hardness testing, Knoop micro-hardness testing, weld zone profile etching, charpy v-notch testing, microstructural characterization, and microscopic joint inspection. All base metal and weld sample test results are given in chapter 4.

3.1 TENSION TESTING.

Tension testing was done in two parts, coupon testing and full section testing. Figure 3.1 shows both types of specimens. Full section tensile testing was incorporated to measure weld tensile capacity. As discussed in chapter 4, circumferential variation was found within welds fabricated at the beginning of the research program. This variation led to the use of full section specimens which test the total weld, rather than just a small sample.



Figure 3.1 Coupon and full section specimens.

3.1.1 Coupon Testing Procedure:

Eight base metal coupons, and three weld coupons were tested. Base metal coupons were obtained from each quadrant of two 3.5" x 0.430" pipe segments. Weld coupons were obtained from two weldments fabricated at the beginning of the research program.

All coupons were fabricated in accordance to subsection S6.2, "Longitudinal Strip Test Specimens", of ASTM A-370 Supplement II- Steel Tubular Products. A 2" gage length was used. Weld coupons were tested with their upset flash in place. All weld planes were located at mid gage length. Adequate gripping was achieved without flattening the grip zones. Testing was conducted using a 120 kip Tinius Olsen universal testing machine. Coupon elongations were recorded using a Tinius Olsen S-1000 extensometer.

Static and dynamic load/elongation readings were taken during each coupon test. As shown in Figure 3.2, static readings were needed to eliminate the effects of dynamic loading on computed material capacity. Static values were obtained by stopping the machine's cross head movement for five minutes.

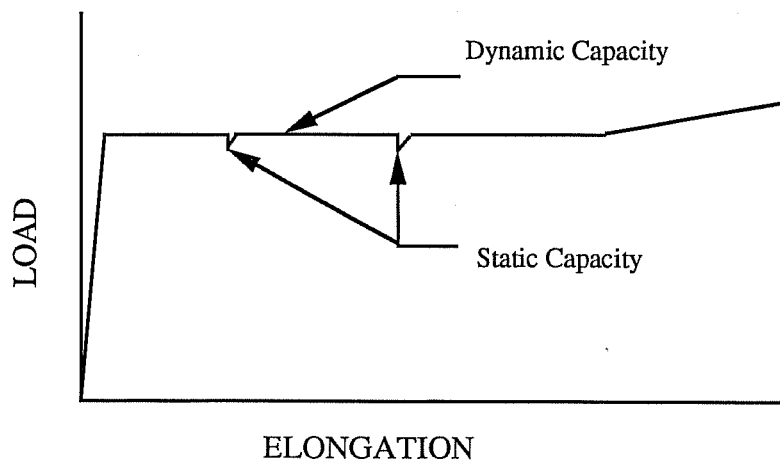


Figure 3.2 Stress-strain curve showing static load readings.

Static and dynamic base metal yield strengths were calculated as shown in Figure 3.2. Yield strengths were not calculated for weld coupons.

3.1.2 Full Section Testing Procedure.

Most welds were tested using full section tensile specimens. One full size base metal specimen was tested to serve as a benchmark for full section weld performance.

A specimen arrangement had to be designed for full section tensile testing. Figure 3.3 shows the adopted configuration. Grip sections made up by 3.75 inch diameter A36 steel rounds were welded to each side of the tensile specimen. Solid rounds were needed to provide adequate strength and solid gripping in the test machine. All pipe to round welds were completed using manual SMAW. E90 Hoballoy 9018M electrodes were used. As shown in figure 3.3, a 37° bevel was used on both the pipe and rounds to achieve good fusion.

The completion of each pipe to round weld took about 45 minutes. This does not include time spent in beveling the joint's ends. Welding the same cross sectional area using homopolar pulse welding takes only a few seconds.

Full section testing was conducted using a 600 kip Satec Systems universal testing machine. A picture of this machine with a specimen in position for testing is shown in Figure 3.4. Relative cross head displacement was measured using a 2" linear potentiometer. Four one inch gage lengths were laid out by a center punch across the weld on each quadrant of the pipe. Elongations across the weld zone and heat affected zone were monitored by these gage marks. Unlike coupon testing, no static load readings were taken. Loading was held at a steady rate until fracture of the specimen.

The ends of each fractured specimen were carefully cut from the grips after testing. Care was taken to avoid damaging the fracture surfaces. These surfaces were then sprayed with a clear acrylic to prevent corrosion. Measurements of gage lengths were then taken, and elongation calculations completed.

The design of the full section testing arrangement allowed the reuse of the steel rounds. Each round had a 400 kip yield capacity, while the pipe's ultimate

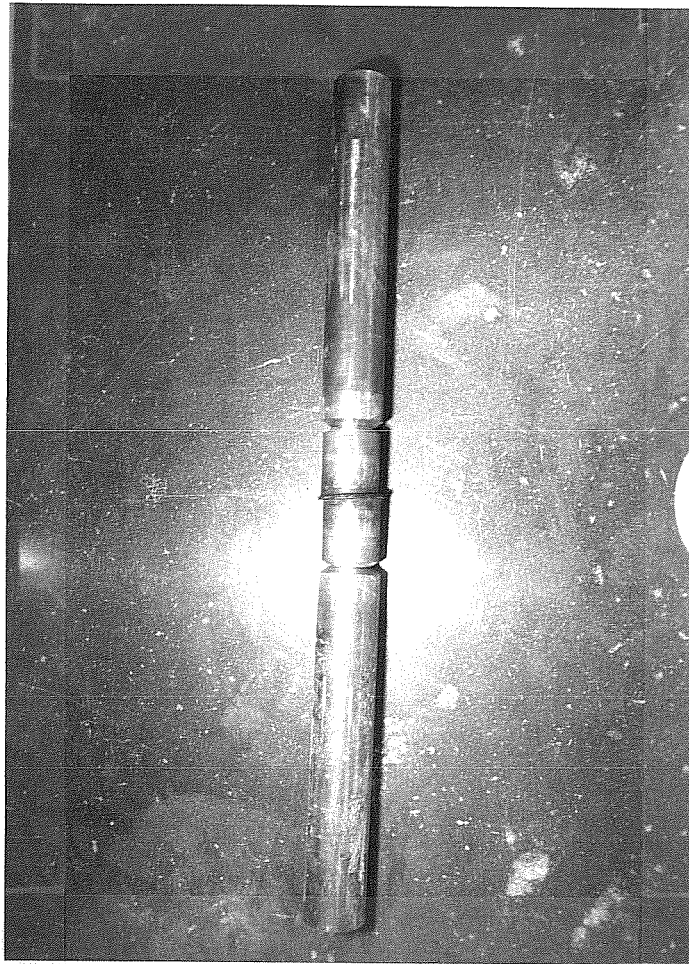


Figure 3.3 Full section specimen

capacity was 350 kips. After separating the fractured pipe from the rounds, the weld connecting the round to the pipe was then machined off. The rounds were then rebevelled, and a new tensile specimen welded.

All but one full section weld specimens were tested with their upset flash left in place. The presence of flash has had at least two effects on the welds' tensile performance. As shown in Figure 3.5, the flash's profile introduced a significant notch into the weld zone. This increased the severity of the tensile test by introducing a stress concentration along the weld line. Second, weld flash acted as weld reinforcement.

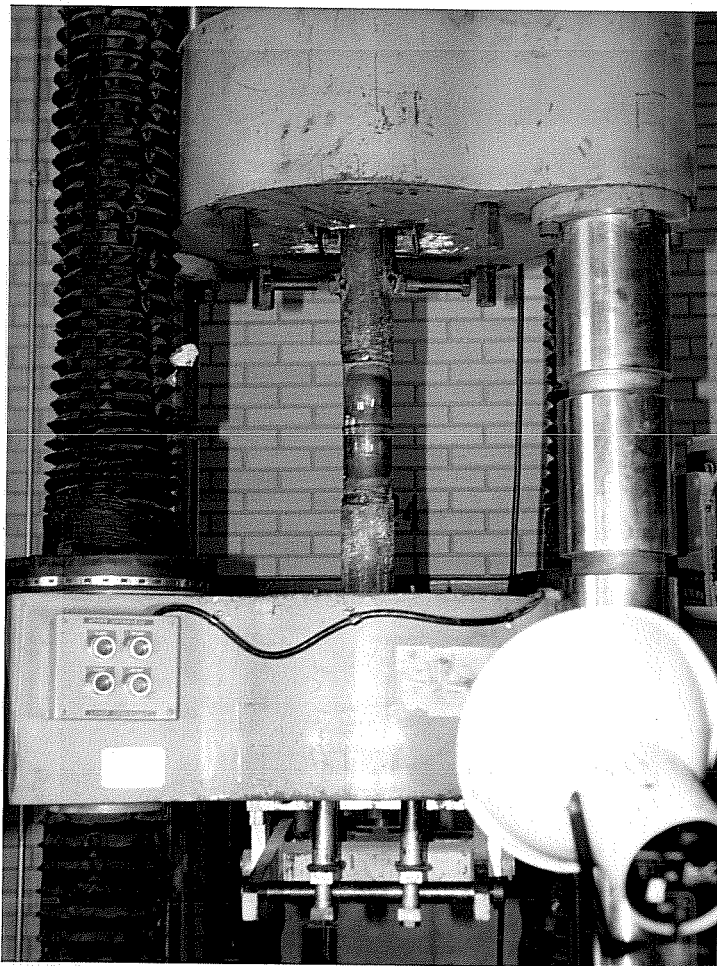


Figure 3.4 Universal testing machine with specimen ready for testing.

One unreinforced weld specimen was tested since API limits the maximum amount of weld reinforcement on pipeline joints. This specimen is shown in Figure 3.6. API limits weld reinforcement to $1/8$ " along the outer pipe wall, and $1/16$ " along the inner wall. The weld's upset flash was machined off using a lathe to meet these requirements.



Figure 3.5 Notch produced by weld flash.

3.2 BEND TESTING.

One strap specimen was subjected to a 180° bend test. This specimen was fabricated in accordance to API Standard 1104, section 2.6.4 “Root and Face Bend Test”. Testing was conducted using a jig specified by API Standard 1104, subsection 2.6.4.2. Root and face reinforcements was removed prior to testing.

Like coupon tensile testing, bend testing was stopped with the discovery of circumferential weld variation. Full section testing gives a better measure of overall weld quality.



Figure 3.6 Unreinforced weld specimen

3.3 CHARPY V-NOTCH TESTING.

To determine the effects of homopolar welding on pipe toughness, base metal specimens and weld specimens were subjected to Charpy V-notch impact testing. Twenty-four base metal specimens were obtained from three 3.5" x 0.430" pipe segments. Twelve weld Charpy specimens were obtained from one weldment. Half of these specimens were designated for weld line testing, the other half for heat affected zone testing.

All Charpy specimens were fabricated in accordance to subsection 20.2.2, "Size and Type", of ASTM A-370 Charpy Impact Testing. Standard type A, 10 x 6.7 mm subsize Charpy specimens were used. These are the largest specimens that can be fabricated considering the size of the pipe's wall thickness, and considering

the possibility of weld misalignment. As shown in figure 3.7, the orientation of the notch on weld charpys followed the orientation of the weld plane. The location of heat affected zone notches was kept at approximately 1/16" away from the weld line. All testing was conducted using a Tinius Olsen Charpy V-Notch tester.

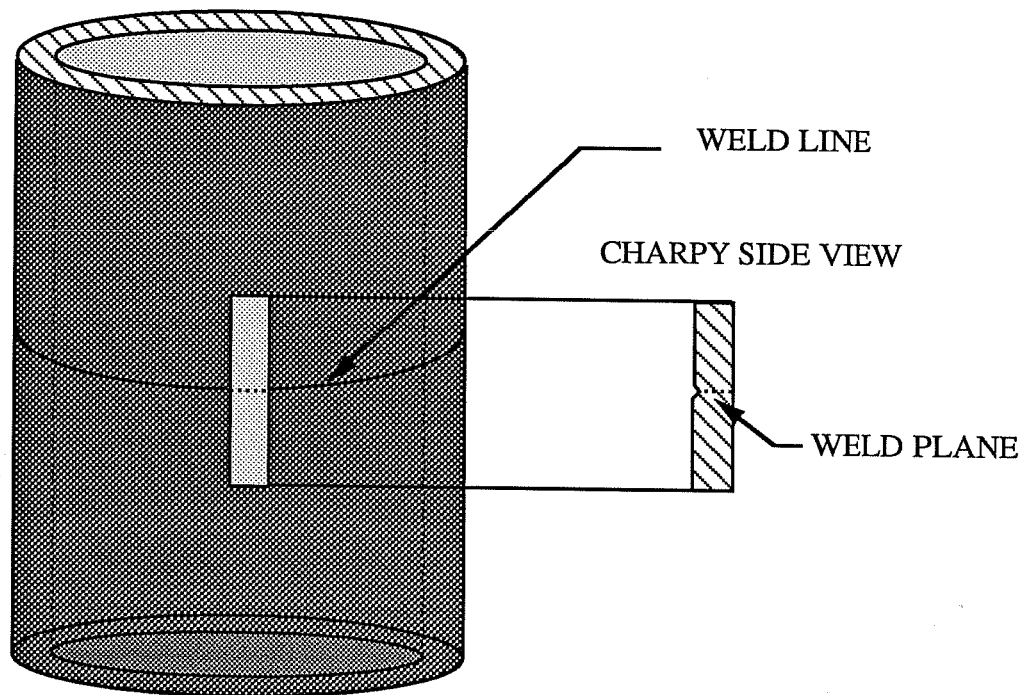


Figure 3.7 Charpy orientation.

Before being notched, the location of the weld line and heat affected zones was found through etching. The etchant solution contained the following:

- 50 gr. Ferric Chloride
- 75 ml. Nitric Acid
- 25 ml. Water

As discussed later, this solution was also used to etch hardness specimens.

3.4 BASE METAL CHEMICAL COMPOSITION.

The chemical composition of the pipes was determined by Chicago Spectro Laboratories Inc. Samples obtained from the grip zone of tested tension coupons were sent for chemical analysis. Results were then compared to Lone Star Steel mill report values.

Table 3.1 shows a summary of the elements tested for during the chemical analysis. As shown, this testing exceeded the minimum required API check for chemical composition. This check is found within section 3, "Chemical Properties and Tests", of API-5L Line Pipe Specifications.

TABLE 3.1 ELEMENTS TESTED FOR DURING BASE METAL CHEMICAL CHARACTERIZATION

ELEMENTS TESTED FOR		MINIMUM REQUIRED API CHECK
C.	Cr.	C.
Mn.	Mo.	Mn.
P.	Al.	P.
S.	V.	S.
Si.	Zr.	Cb.
Cu.	Nb.	V.
Ni.	Ti.	Ti.
Al.	N.	
B.		

Table 3.1 Base metal chemical characterization.

3.5 ULTRASONIC WELD SURVEYS.

Most weldments were subjected to extensive ultrasonic testing. An Applied Industries UJ Reflectoscope was used in conjunction with a 5mhz, 0.25" diameter, compression wave transducer to examine the welds. Adequate transducer coupling was achieved using oil.

As shown in Figure 3.8, weld quality was monitored using longitudinal weld surveys. Several steps were involved in completing these tasks. First, an ultrasonic reference level was set using the side drilled hole in a standard IIW calibration

block. The pipe ends and the transducer face were then coated with oil to provide good coupling. A gain level was then set for the pipe sample. The strength of the transducer signal was increased until obtaining a good reflection from the end of the pipe. Weld surveys were then conducted by carefully moving the transducer along the pipe's circumference. The location of flaws, and their respective gain levels, were recorded. Flaw ratings were then calculated by subtracting the reference flaw level. Welds with large defects were not subjected to further testing.

Cross sectional maps of welds showing small defects were then made. These maps, such as the one shown in Figure 3.9, were then compared to the specimen's tensile failure surface.

3.6 MACRO-HARDNESS CHARACTERIZATION.

Macro-hardness testing was conducted to determine the hardness properties of homopolar welds. Testing was done using a Wilson Rockwell Series 500 Hardness Tester. All measurements were made using the Rockwell "B" scale.

Welds fabricated at the beginning of the research project were subjected to circumferential and longitudinal hardness testing. As shown in Figure 3.10, hardness specimens were taken from all four pipe quadrants. Circumferential hardness testing was stopped with the incorporation of full section tensile testing. Only one hardness coupon was obtained for these welds.

Figure 3.11 shows the dimensions of a typical hardness specimen. The length of most samples was kept between 2.5" and 3". Longer samples were not required since the ends of these specimens already showed base metal hardness levels. Most specimens were 1" wide. This was the largest width that provided flat testing surfaces. Note, since most of the tested pipes failed along the weld line, one of the specimens' ends contained the weld plane.

The fabrication of hardness specimens was completed in several steps. First coupons were carefully cut, milled, and ground. Efforts were made to obtain the best possible surface finish. Each specimen was then lightly etched using the solution described above to locate the weld line and heat affected zones. After being etched, photographs of the hardness specimens were taken. Figure 3.12 shows a typical

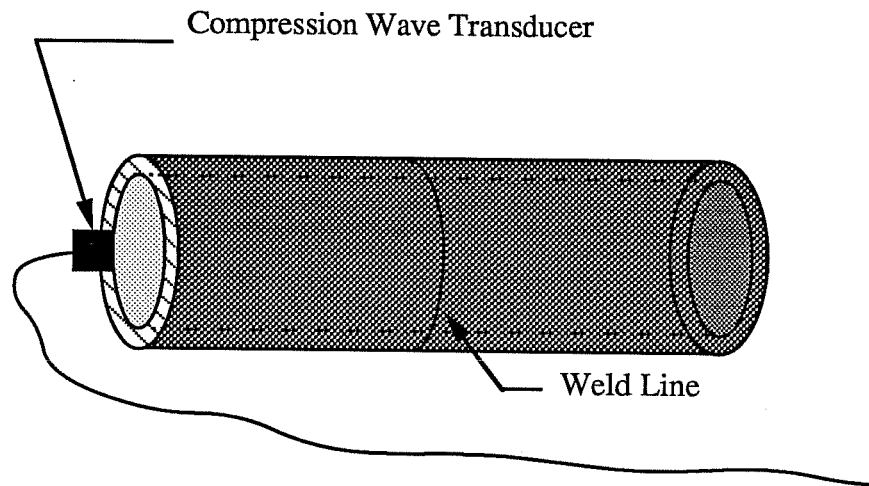


Figure 3.8 Longitudinal ultrasonic weld survey.

DETECTED FLAWS - 36 Db GAIN LEVEL

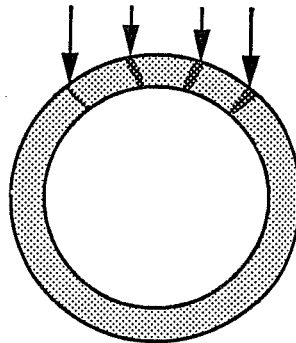


Figure 3.9 Cross sectional ultrasonic map.

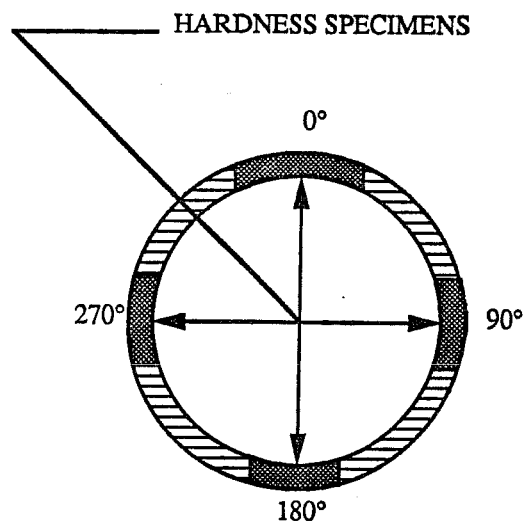


Figure 3.10 Location of samples used for circumferential hardness characterization.

photograph. The specimens were then reground. Hardness readings were not taken on the etched surface due to pitting produced by the etchant solution.

The location of the weld line and heat affected zone was marked on the reground specimens by using the etch photographs. As shown in Figure 3.13, hardness points were then mapped along each sample. The distance between measurements varied according to their relative distance from the weld line. Longitudinal hardness readings were taken on the mapped points using the hardness tester.

In addition to longitudinal hardness testing, through thickness and weld line hardness measurements were taken on each hardness specimen. Hardness profiles were constructed from the gathered data. Each tested specimens was then reetched to validate these hardness profiles with respect to the weld's microstructure.

TYPICAL HARDNESS SPECIMEN DIMENSIONS

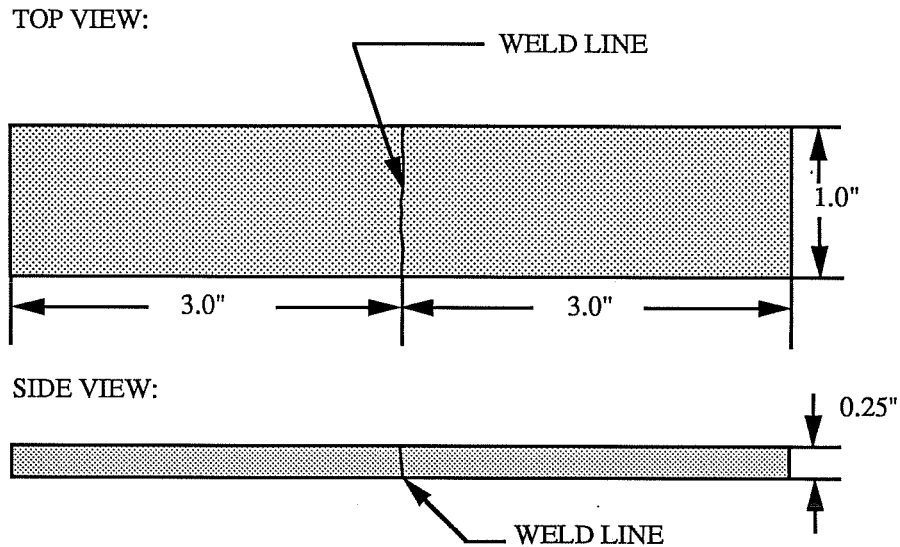


Figure 3.11 Hardness specimen dimensions.

3.7 MICRO-HARDNESS CHARACTERIZATION.

One weldment was subjected to Knoop micro-hardness testing. All micro-hardness testing was conducted at Vetco Gray Inc. Knoop readings were taken up to ± 0.35 " away from the weld line. Reported results were then compared to macro-hardness values taken along the same weldment.

3.8 WELD ZONE PROFILE ETCHING.

As mentioned above, hardness and charpy specimens were lightly etched before being tested. Care was taken to insure good etches. Allowing the reaction to continue too long results in severely stained samples. Subtle changes in microstructure cannot be noticed when this occurs. Samples which showed too strong an etch were reground and reetched.

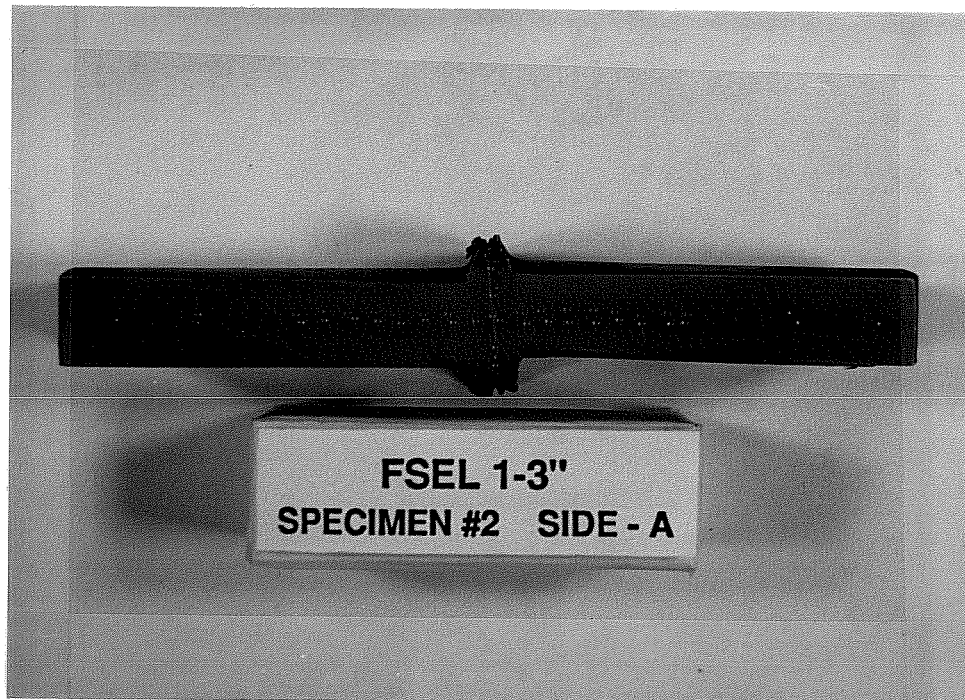


Figure 3.12 Etched hardness specimen.

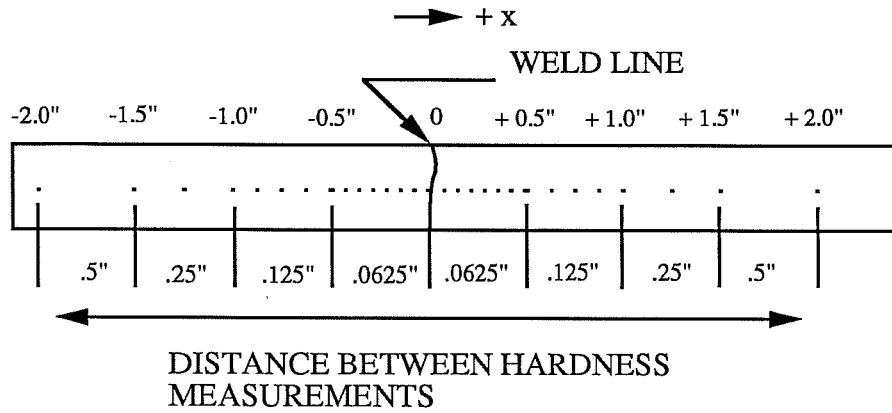
3.9 MICROSTRUCTURAL CHARACTERIZATION.

Samples from two different weldments and from the base metal were subjected to microstructural characterization. Micrographs of the weld line, the heat affected zone, and the base metal were taken. 100X and 400X magnifications were used. Changes in microstructure were identified through the use of these micrographs. All microstructural work was done at Vetco Gray Inc.

3.10 JOINT SURFACE RESISTANCE TESTING.

Work dealing with the effects of end preparation on homopolar surface resistance was done. Testing was performed on seven different end preparations. These include: a rough band saw cut finish, three machined rough finishes, and three wire mesh surface inserts. All work was done at Vetco Gray Inc.

LONGITUDINAL HARDNESS READINGS.



WELD LINE HARDNESS READINGS.

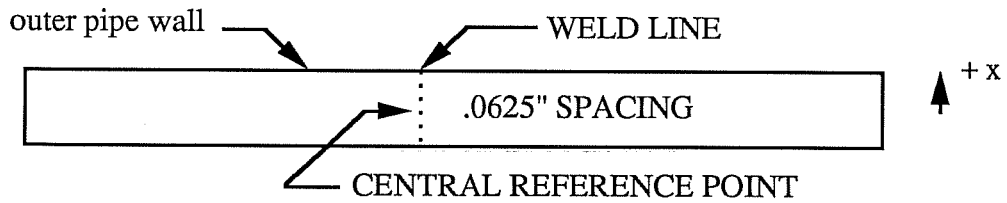


Figure 3.13 Map for longitudinal hardness testing.

CHAPTER 4

TEST RESULTS

This chapter presents a comprehensive summary of results obtained during the investigation of homopolar pulse weldments. Forty eight welds have been fabricated to date, welds 2.01 through 2.48. Of these, only those welds displaying acceptable visual characteristics were tested. Samples showing excessive lateral displacement, showing no observable upset, or showing obvious lack of fusion were not tested. A summary of tests performed on each of the tested weldments is given in Table 4.1.

Table 4.2 lists the production parameters used for each tested weld. As mentioned in chapter two, several parameters significantly affect the quality of the final weldment. Among these are generator discharge speed, initial pressure, upset pressure, and upset time. These variables affect the welding process in the following manner. Generator speed controls the level of energy that goes into the weld. Initial pressure is required to provide enough surface resistance for interface heat generation. Upset pressure is needed to forge the pipes together once enough heat is generated. Upset time controls the duration of interface heat generation. What sets generator speed, initial pressure, upset pressure, and upset time apart from other factors affecting weld quality is that these parameters are directly preprogrammed by the controller before each weld. Although lack of welding control has prevented a complete evaluation of their relative importance, this chapter presents brief discussions on their effects. During this research the welder's hydraulic system was modified to achieve better load control. The incorporation of a closed loop servo-controlled system significantly affected weld quality. Because of this, some sections in this chapter are separated into two parts; discussion of results before and after the hydraulic modification. Welds 2.01 through 2.30 were fabricated before the hydraulic modification; welds 2.31 through 2.48 were fabricated after the hydraulic modification.

Finally, one section is dedicated to the effects of post weld heat treatment on homopolar welds.

TABLE 4.1 SUMMARY OF TESTS CONDUCTED TO DATE

TEST:	TEN	UT	HARD	ETCH	CVN	BEND
WELD 2.08	X	X	X	X	X	
WELD 2.11	X	X	X	X		X
WELD 2.21*	X		X	X		
WELD 2.22			X			
WELD 2.24*	X	X	X	X		
WELD 2.25**		X				
WELD 2.26*	X	X	X	X		
WELD 2.27*	X	X	X	X		
WELD 2.29*	X	X	X	X		
HYDRAULIC OVERHAUL						
WELD 2.31*	X	X				
WELD 2.34*	X					
WELD 2.35*	X					
WELD 2.36*	X					
WELD 2.39*	X					
WELD 2.40*	X					
WELD 2.42*	X					
WELD 2.47*	X					
WELD 2.48*	X					

* Welds designated for full section tension testing.

** Welds whose poor ultrasonic performance justified no additional testing.

Table 4.1 Summary of tests conducted to date.

TABLE 4.2 SUMMARY OF WELD PARAMETERS USED

WELD #	DISCHARGE SPEED (rpm)	Pinit/ Pupset	UPSET TIME
2.08	3000	8/30	0.80
2.11	2800	8/20	0.80
2.21	2800	4/30	0.35
2.22	3000	4/30	0.47
2.24	3000	4/30	0.47
2.25	3000	4/na	na
2.26	3000	4/30	1.00
2.27	3000	4/30	1.00
2.29	3000	4/30	1.00
HYDRAULIC OVERHAUL			
2.31	3000	5/30	0.50
2.34	2700	5/30	0.50
2.35	3000	5/25	0.50
2.36	3000	5/25	0.50
2.39	3000	5/25	0.50
2.40	3000	5/25	0.50

- * Discharge speed given in terms of generator's rpm's.
- ** Pinit/Pupset given in ksi.
- *** Upset times given in secs.
- na Values not available.

Table 4.2 Summary of weld parameters used.

4.1 BASE METAL PROPERTIES.

The effects of the homopolar welding process have been quantified by referencing weld results to base metal properties. A complete characterization of the base metal was completed at the beginning of the homopolar research program. Tables 4.3, 4.4, and 4.5, and Figure 4.1 show results obtained through this characterization. Table 4.3 summarizes the base metal's tensile properties in terms of coupon testing.

Table 4.4 summarizes the base metal's tensile properties in terms of full section testing. Table 4.5 summarizes the base metal's chemical composition. Figure 4.1 shows the base metal's charpy v-notch test data. Like weld testing, all base metal testing procedures are described in chapter three.

TABLE 4.3 BASE METAL TENSILE RESULTS- COUPON TESTING

	LABORATORY	MILL
STATIC YIELD STRENGTH:		
HIGH VALUE	48.5 ksi	
LOW VALUE	44.3 ksi	
AVERAGE	46.3 ksi	na
STD DEV	1.45	
DYNAMIC YIELD STRENGTH:		
HIGH VALUE	49.2 ksi	
LOW VALUE	46.7 ksi	
AVERAGE	47.9 ksi	60.0 ksi
STD DEV	0.86	
ULTIMATE CAPACITY:		
HIGH VALUE	87.0 ksi	
LOW VALUE	79.8 ksi	
AVERAGE	84.9 ksi	85.1 ksi
STD DEV	2.24	
% ELONGATION:		
HIGH VALUE	36.7%	
LOW VALUE	30.0%	
AVERAGE	33.4%	na
STD DEV	2.57	

* Coupons prepared according to ASTM A-370 specifications.

** na- Values not available.

Table 4.3 Base metal tensile capacity - Coupon results.

Table 4.3 summarizes the results obtained through base metal coupon tensile testing. Values for average, highest, and lowest coupon capacities are reported in this table. In addition, values for standard deviation were calculated from the collected data. Note that a difference exists between average laboratory and mill report yield strengths. This may be attributed to differences in test loading rates and test procedures. Ultimate capacities do agree.

Table 4.4 shows a summary of full section base metal tensile capacities. Since full section tensile capacities were not provided in the mill report, only laboratory results are reported in Table 4.4.

TABLE 4.4 FULL SECTION BASE METAL TENSILE CAPACITY

LABORATORY	
DYNAMIC YIELD STRENGTH:	49.7 ksi
ULTIMATE CAPACITY:	83.5 ksi
% ELONGATION	39.5%

* No full section capacities were supplied in the mill report.

Table 4.4 Full section base metal tensile capacity.

Table 4.5 summarizes the base metal's chemical composition. The amount of elements for which the pipes were tested for exceeded the minimum required chemical check found in API 5L - Line Pipe Specifications.

The most important result shown in table 4.5 is the material's high carbon content. A carbon content of 0.36% is too high for most industrial standards due to the problems it may pose in terms of weldability. Showing that homopolar welds can be made using this steel will help in establishing the merits of homopolar welding for marine pipeline construction.

Figure 4.1 shows the charpy v-notch test results for the base metal. This data was obtained through the testing of twenty four charpy v-notch specimens. As mentioned in chapter three, standard type A, 10 x 6.7 mm. subsize specimens were used.

TABLE 4.5 BASE METAL CHEMICAL COMPOSITION

	TESTED	MILL
ELEMENT:		
C.	0.35%	0.35%
Mn.	0.67%	0.65%
P.	<0.005%	0.04%
S.	0.019%	0.05%
Si.	0.09%	na
Cu.	0.16%	na
Ni.	0.07%	na
Cr.	0.10%	na
Mo.	0.03%	na
Al.	0.020%	na
V.	<0.005%	na
Zr.	<0.005%	na
Nb.	<0.005%	na
Ti.	<0.005%	na
N.	0.0091%	na
B.	<0.0005%	na

Table 4.5 Base metal chemical composition.

4.2 WELD TENSILE TESTING RESULTS.

Table 4.6 summarizes all weld tensile results obtained to date. Specimens that experienced a weld line fracture are referenced by the label "wl". Specimens with a base metal failure are referenced by the label "bm". Also note, weld 2.36 is labeled "ur". This weld was tested after having its weld reinforcement machined off.

Results shown in Table 4.6 were compiled through the use of both ASTM strap coupons and full section tensile specimens. Coupon capacities were calculated using the measured reduced section area. Full section capacities were calculated using the pipe's measured cross sectional area. To do this, specimen cross sectional dimensions were recorded before each test. The presence of weld reinforcement was not considered in either coupon or full section strength calculations. Coupon elongations were calculated using a 2" gage length. Full section elongations were

3.5" x 0.430" PIPE
 BASE METAL CHARACTERIZATION

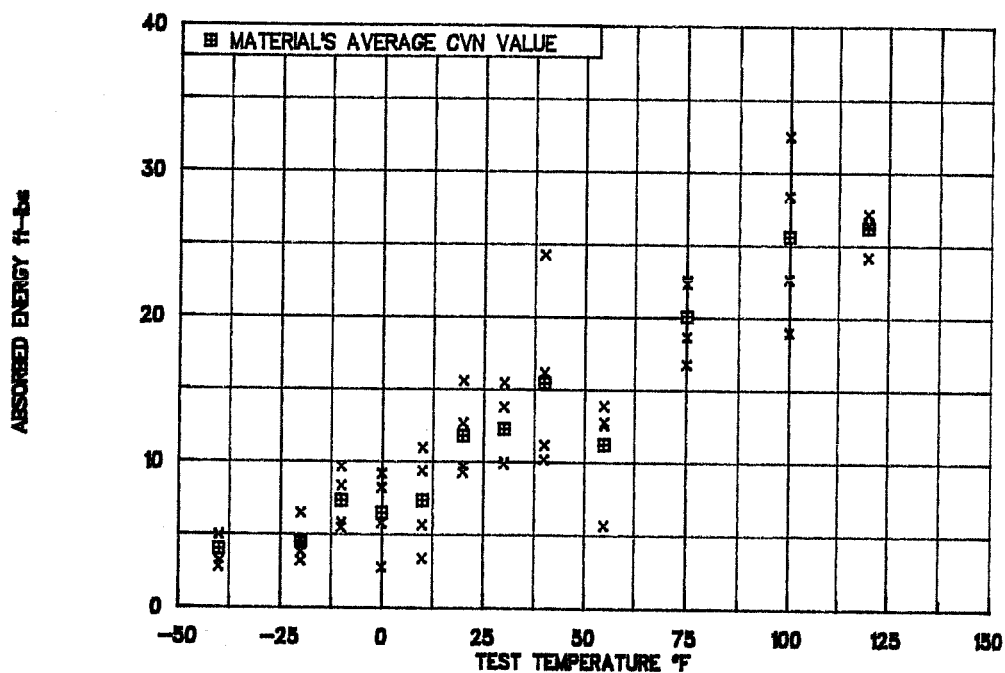


Figure 4.1 Base metal charpy v-notch data.

obtained by averaging the elongations across each quadrant of the pipe. Quadrant elongations were obtained using four one inch gage lengths across the weld and heat affected zone.

As shown in Table 4.6, the performance of each weld is referenced to the base metal capacity. Welds which failed at loads lower than the base metal's ultimate capacity, or who fractured along the weld plane, are considered unacceptable production-type welds. Production-type welds represent welds that would be acceptable under normal industrial standards. Results in Table 4.6 indicate that the changes in the hydraulic system improved weld quality since all successful welds occurred after the overhaul.

TABLE 4.6 SUMMARY OF WELD TENSION TEST RESULTS

WELD	ULTIMATE CAPACITY*	% ELONG	ACCEPT
WELD 2.08 **	78.6 ksi - ws	5.0%	
WELD 2.11 **	86.2 ksi - bm	15.0%	
WELD 2.11 **f	66.2 ksi - ws	2.5%	
WELD 2.21 ***	68.3 ksi - ws	na	
WELD 2.24 ***f	2.0 ksi - ws	0.0%	
WELD 2.26 ***	83.6 ksi - ws	9.4%	
WELD 2.27 ***	65.3 ksi - ws	1.6%	
WELD 2.29 ***	64.0 ksi - ws	2.5%	
HYDRAULIC OVERHAUL			
WELD 2.31 ***	84.9 ksi - bm	10.0%	x
WELD 2.34 ***	56.5 ksi - ws	na	
WELD 2.35 ***	85.1 ksi - bm	12.8%	x
WELD 2.36 ***	86.2 ksi - bm/ur	18.0%	x
WELD 2.39 ***	71.1 ksi - ws	2.8%	
WELD 2.40 ***	88.6 ksi - bm	21.6%	x
WELD 2.42 ***	87.1 ksi - bm	17.0%	x
WELD 2.47 ***	85.2 ksi - bm	22.9%	x
WELD 2.48 ***	86.2 ksi - bm	29.5%	x
Base Metal **	84.9 ksi	33.4%	
Base Metal ***	83.5 ksi	39.5%	

- * Strength calculations are based on nominal base metal area.
- ** Coupons fabricated according to ASTM A370 Supplement II - Steel Tubular Products.
- *** Full section tension specimens.
- bm Failure occurred in the base metal, and away from the weld zone.
- ws Failure occurred along the weld surface.
- ur Unreinforced tension specimens.
- f Flaws were detected prior to testing through Ultrasonic testing.
- ACCEPT - Specimens who fractured away from the weld line after having developed base metal capacities.

Table 4.6 Weld tension test summary.

4.2.1 TENSION RESULTS - Welds made before hydraulic overhaul.

As shown in Table 4.6, almost all welds fabricated before the hydraulic overhaul showed a poor tensile performance. Welds 2.08, 2.11, 2.21, 2.24, 2.27, and 2.29 fractured at the weld surface before reaching the base metal's tensile strength. In addition, all these samples experienced very brittle failures. The average coupon elongation was 7.5%, while the average full section elongation was 1.7%. This performance is very poor when compared to the 33.4% coupon, and the 39.5% full section base metal elongations.

A reflection of weld brittleness is shown by the specimens' fracture surfaces. As shown in Figure 4.2, very flat fracture surfaces were formed by these welds. It is clear that limited material diffusion between pipes led to the formation of well defined, low quality weld planes. The presence of flat fracture surfaces suggests that insufficient interface heating occurred before to the application of upset load.

In addition to surface flatness, poor bonding was found along the circumference of welds 2.08, 2.11, 2.24, and 2.25. Figure 4.3 shows a cross sectional map constructed for weld 2.11. As shown, lack of fusion extended through a significant portion of this weld. Similar flaws were found in welds 2.08, 2.24, and 2.25. The presence of these flaws shows that interface heating was not homogeneous around the cross section. As discussed later, pipe misalignment, or variations in stiffness within the welding fixture may have played a role in the forming of such defects. The presence of circumferential variation required the use of full section tensile specimens. As shown in Figure 4.3, coupons provide measures of local quality. Evaluations of overall weld quality can only be achieved through full section testing.

Lack of fusion was also found along the inner wall of welds 2.11, 2.24, 2.27, and 2.29. Figure 4.4 shows a photograph of weld 2.29. As shown, these defects run along most of the joint's inner wall surface, and extend through approximately one fifth of the pipe's wall thickness. As discussed later, radial flaws could not be detected through normal ultrasonic techniques.

The presence of radial flaws along the inner pipe wall has raised questions concerning the nature of the weld's heating process. These flaws indicate that interface heating first concentrates along the pipes' outer region. As the welding process



Figure 4.2 Fracture surface of weld fabricated before hydraulic modification.

continues, heat generation seems to transfer through the pipes' wall thickness and into the inner wall region. A reduction of surface resistance along the outer wall, or local melting may act as catalysts for this heat transfer. If insufficient surface heating is applied, however, heat generation will stay along the outer region without transferring into the inner wall region, therefore resulting in the formation of inner wall radial flaws. Up to this now it was assumed that the heating process was

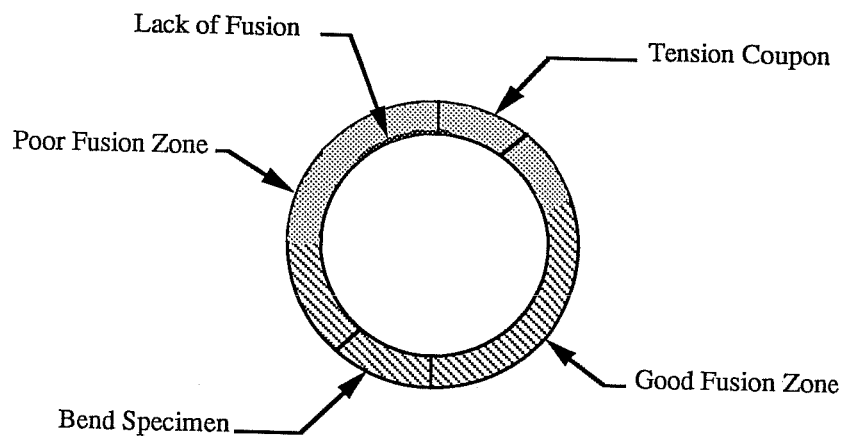


Figure 4.3 Ultrasonic cross sectional map of weld 2.11.

homogeneous across the joint's interface. It appears that this assumption must be reevaluated.

Only one early weld was able to develop the base metal's tensile capacity. As shown in Table 4.7, weld 2.26 fractured at the weld surface after reaching a tensile strength of 83.6 ksi and an elongation of 9.4%. Although it cannot be considered an acceptable production type weld since it fractured along the weld plane, results obtained from this weld were considered encouraging. Because of this, weld 2.29 was fabricated as a duplicate of weld 2.26 to address two questions; to see if the system is capable of reproducing welds, and to see whether fracture would occur away from the weld line.

As shown in Table 4.7, welds 2.26 and 2.29 were produced using the same apparent set of welding parameters. These welds, however, behaved in totally different manners. Weld 2.29 failed to develop the base metal tensile capacity.

It was found, after going back through the parameter traces for welds 2.26 and 2.29, that lack of hydraulic control may have led to the difference in tensile performance. Figure 4.5 shows the pressure profiles for welds 2.26 and 2.29. It is



Figure 4.4 Lack of fusion along inner wall - Weld 2.29.

clear that these profiles do not match. The initial pressure for weld 2.29 was lower than the initial pressure for weld 2.26. As mentioned before, initial pressure has a direct effect on surface resistance. By having a lower initial pressure, weld 2.29 had lower surface resistance, thus lower interface heat generation. To further the potential for inadequate bonding, final upset pressure for weld 2.29 was lower than final upset pressure for weld 2.26. It is clear that lack of pressure control affected the quality of these welds.

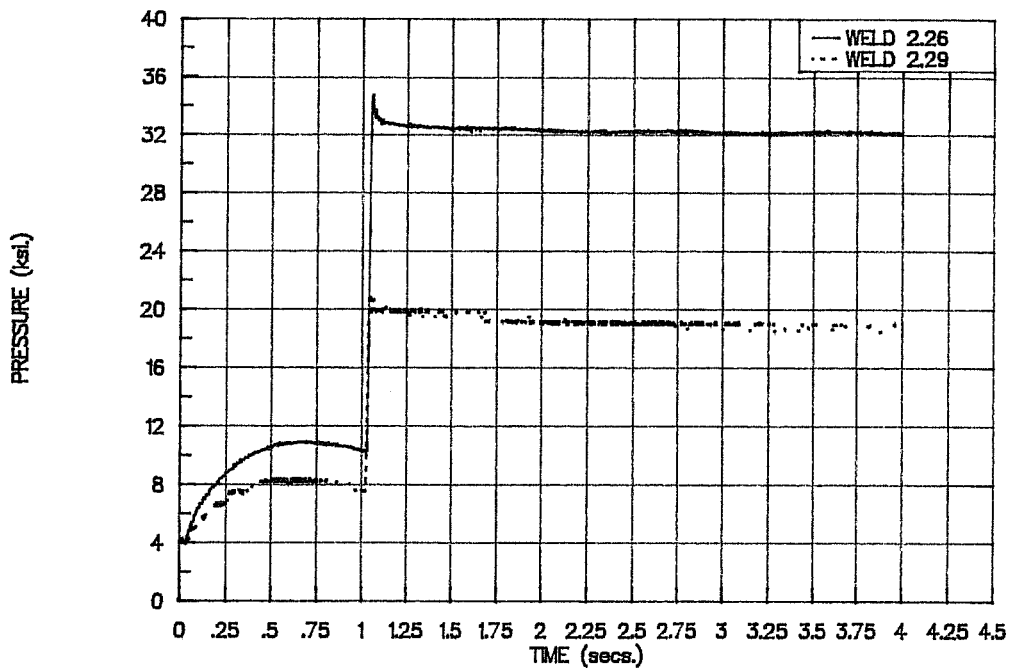
TABLE 4.7 BEHAVIOR OF IDENTICAL WELDS

WELD PARAMETERS USED	WELD 2.26	WELD 2.29
Discharge Speed (rpm)	3000	3000
Pinitial/Pupset (ksi)	4/30	4/30
Time of Upset (sec)	1.0	1.0
Peak Current (kA)	306	315
TENSILE PERFORMANCE:		
ULTIMATE CAPACITY (ksi)	83.6	64.0
% ELONGATION	9.4%	2.5%

Table 4.7 Behavior of "identical" welds.

The servo-controlled system was installed to remove lack of hydraulic control as a factor affecting weld quality. Figure 4.6 shows two pressure traces; one corresponding to a weld fabricated before the hydraulic overhaul, and one corresponding to a weld fabricated after the hydraulic overhaul. The pre-hydraulic modification profile shows that the initial pressure level drifted upward before the application of upset load. Initial pressure drifting may be attributed to pipe thermal expansion. The presence of drifting may have resulted in a loss of surface resistance which then lowered the potential for heat generation. This would explain why low interface material diffusion, and why radial flaws were present in welds fabricated before the hydraulic modification. As shown in Figure 4.6, better initial pressure control was achieved with the new hydraulic system.

PRESENCE OF PRESSURE VARIATION
 WELDS 2.26 AND 2.29 - ASSUMED "IDENTICAL WELDS"



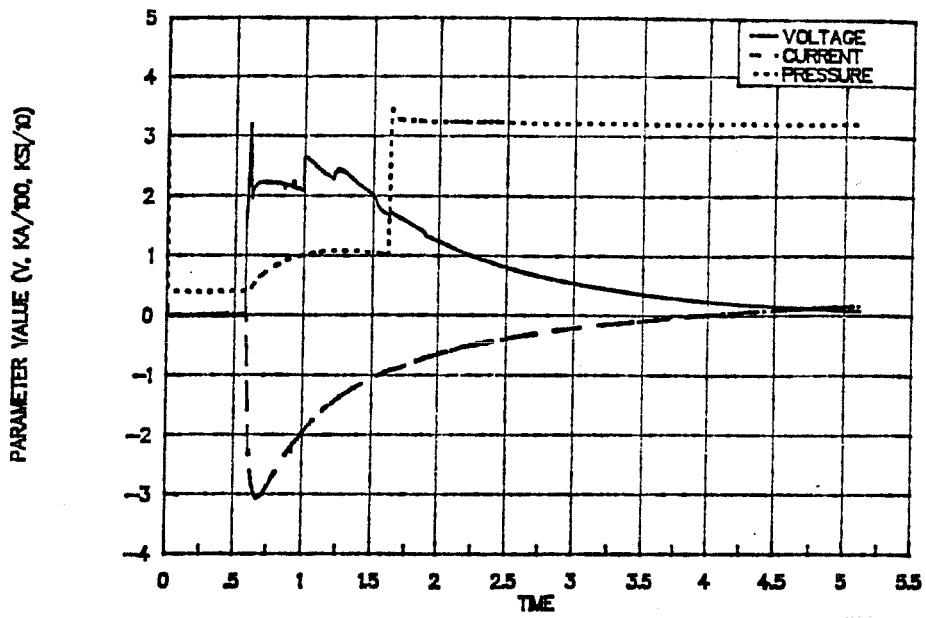
1.0 UPSET TIMES WERE USED ON BOTH WELDS

Figure 4.5 Comparison of weld pressure profiles - Welds 2.26 and 2.29.

4.2.2 TENSION RESULTS - Welds made after hydraulic overhaul.

Table 4.8 shows tensile results for welds produced after the hydraulic overhaul. It is clear that the welds' tensile behavior improved with the incorporation of the closed loop hydraulic system. Seven out of nine specimens fractured away from the weld zone after having developed the base metal's tensile capacity. Only welds

BEHAVIOR OF WELD PARAMETERS
WELD 2.26



NSF 2.37

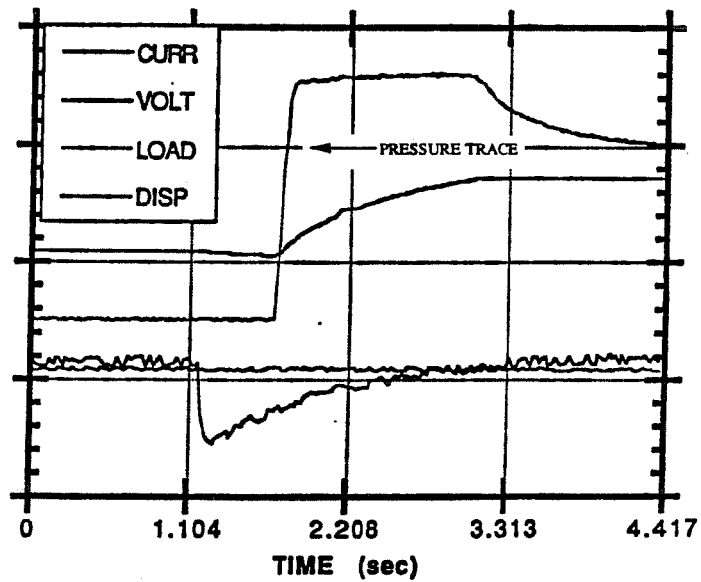


Figure 4.6 Comparison of pressure profiles made before and after the hydraulic modification.

**TABLE 4.8 TENSILE PERFORMANCE OF WELDS
MADE AFTER HYDRAULIC OVERHAUL**

WELD	ULTIMATE CAPACITY*	% ELONG
WELD 2.31 **	84.9 ksi - bm	10.0%
WELD 2.34 **	56.5 ksi - ws	na
WELD 2.35 **	85.1 ksi - bm	12.8%
WELD 2.36 **	86.2 ksi - bm/ur	18.0%
WELD 2.39 **	71.1 ksi - ws	2.8%
WELD 2.40 **	88.6 ksi - bm	21.6%
WELD 2.42 **	87.1 ksi - bm	17.0%
WELD 2.47 **	85.2 ksi - bm	22.9%
WELD 2.48 **	86.2 ksi - bm	29.5%
Base Metal **	83.5 ksi	39.5%

- * All strength calculations are based on nominal base metal area.
- ** Full section tension specimens.
- bm Failure occurred in the base metal, and away from the weld zone.
- ws Failure occurred along the weld surface.
- ur Specimens whose weld reinforcement was milled off.

Welds that were not tested experienced excessive lateral displacement.

Table 4.8 Tensile performance of welds made after the hydraulic overhaul.

2.34 and 2.39 failed to perform in this manner. Figure 4.7 shows a specimen that passed the tension test.

In addition to improved strength, specimens fabricated after the hydraulic modification showed an improvement in weld ductility. The average elongation experienced by welds 2.31, 2.35, 2.36, 2.40, 2.42, 2.47, and 2.48 was 18.8%. This compares favorably to the 9.4% elongation shown by weld 2.26. As mentioned in

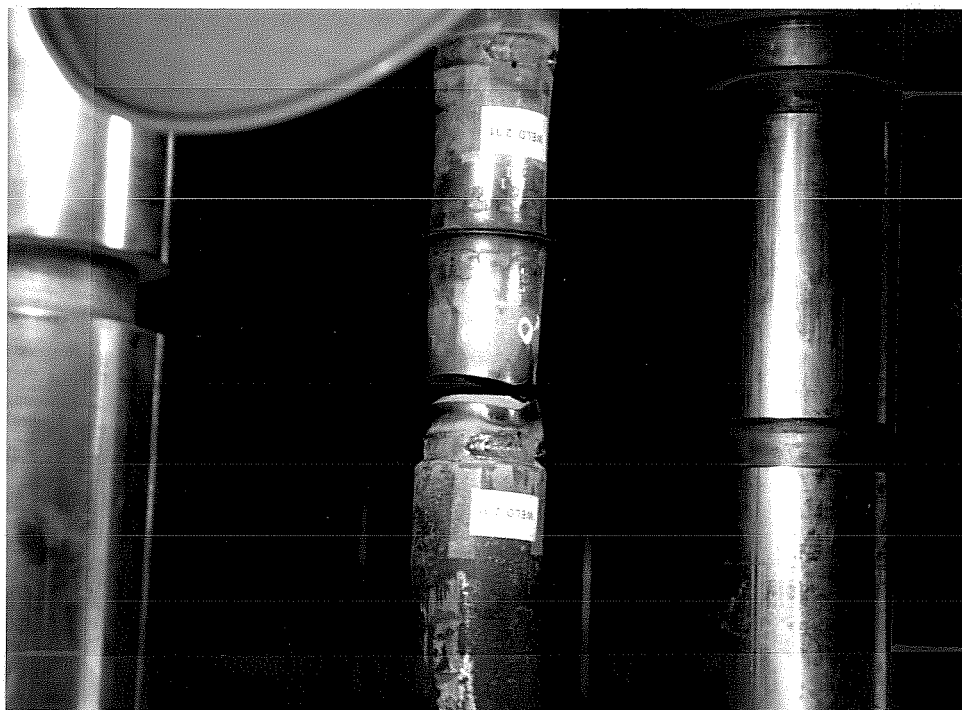


Figure 4.7 Specimen that passed the tensile test.

the last section, weld 2.26 was the only weld made before the hydraulic modification capable of reaching the base metal's strength.

Weld reproducibility has also increased with the incorporation of a closed loop hydraulic system. Welds 2.31, 2.35, and 2.36 were fabricated using the same set of initial parameters; discharge speed - 3000 rpm, initial load - 5.0 ksi, upset load - 25.0 ksi, and time of upset - 0.5 sec. All these samples fractured away from the weld zone after having developed the base metal tensile capacity. Improvements in weld reproducibility may be attributed to better pressure control. Better pressure control

promotes the maintenance of higher and more controlled surface resistance. It is not known, however, whether other mechanical/electrical problems, such as improper press alignment, inadequate fixture stiffness, or unpredicted current distributions may also be affecting the reproducibility of welds.

One additional result should be noted. As shown in Table 4.8, weld 2.36 developed the base metal tensile capacity. The importance of this result lies in the fact that this weld's reinforcement was machined off prior to being tested. Figure 4.8 shows weld 2.36 after being tested. Failure occurred away from the weld zone even though improper pipe alignment was present. This result is encouraging in terms of the applicability of homopolar welding in laying operations. Weld 2.36 has shown that unreinforced homopolar welds are capable of developing base metal strengths.



Figure 4.8 Weld 2.36 after being tested.

Results obtained from welds made after the hydraulic overhaul are encouraging. Two significant problems must now, however, be addressed. First, the fracture of welds 2.31, 2.35, 2.36, 2.40, 2.42, 2.47, and 2.48 initiated at points of electrical contact. Stress concentrations produced by local hard spots may be promoting the occurrence of fracture at these locations. Although this problem can be eliminated through the application of post weld heat treatment, local arcing is undesirable and should be avoided. In addition, copper inclusions were deposited on the outer pipe wall. The presence of these inclusions may lead to the degradation of sample ductility. Steel shim conductors placed between the pipe and the electrodes have been used to eliminate this problem. Welds 2.30, 2.47, and 2.48, were welded using these shims. Although the deposition of inclusions may have been eliminated, local arcing occurred between the pipes, shims, and electrodes.

4.3 BEND TEST RESULTS.

One strap bend test was conducted. A sample was taken from weld 2.11 and fabricated in accordance to API Standard 1104, section 2.6.4 "Root an Face Bend Test". This sample was then tested using a jig specified by subsection 2.6.4.2 of API Standard 1104.

As shown in Figure 4.9, the weld was able to undergo large deformations. This figure shows the specimen after its sides were machined and ground.

Additional bend testing was not conducted due to the presence of circumferential weld variation. It is felt that full section testing provides a better measure of overall weld quality than either coupon tensile testing or bend testing.

4.4 ULTRASONIC TESTING RESULTS.

Most welds were subjected to ultrasonic inspection. The applicability of ultrasonic testing was examined by carefully mapping flawed specimens. These maps were then compared to the specimens' fracture surfaces after being tensile tested.

Figure 4.10 shows an ultrasonic map constructed for weld 2.21 and its corresponding fracture surface. As shown, the map predicted fairly well the specimen's



Figure 4.9 Tested bend specimen.

failure surface. Both lack of fusion and weld inclusions were picked up during the ultrasonic inspection.

Only tight flaws running along the inner or outer wall perimeters, such as those shown in Figure 4.11, were difficult to detect using ultrasonic equipment. Two reasons may explain this. All welds were inspected with their flash reinforcement on. Reinforcement reflections hid the reflection signal produced by peripheral flaws. In addition, only longitudinal compression wave transducers were used. Using 45° or

DETECTED FLAWS - 36 Db GAIN LEVEL

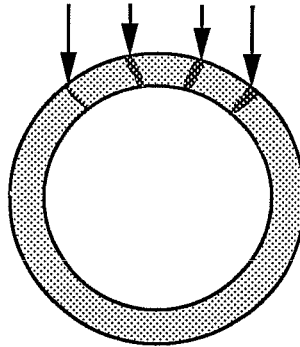


Figure 4.10 Comparison of ultrasonic evaluation and specimen fracture surface.

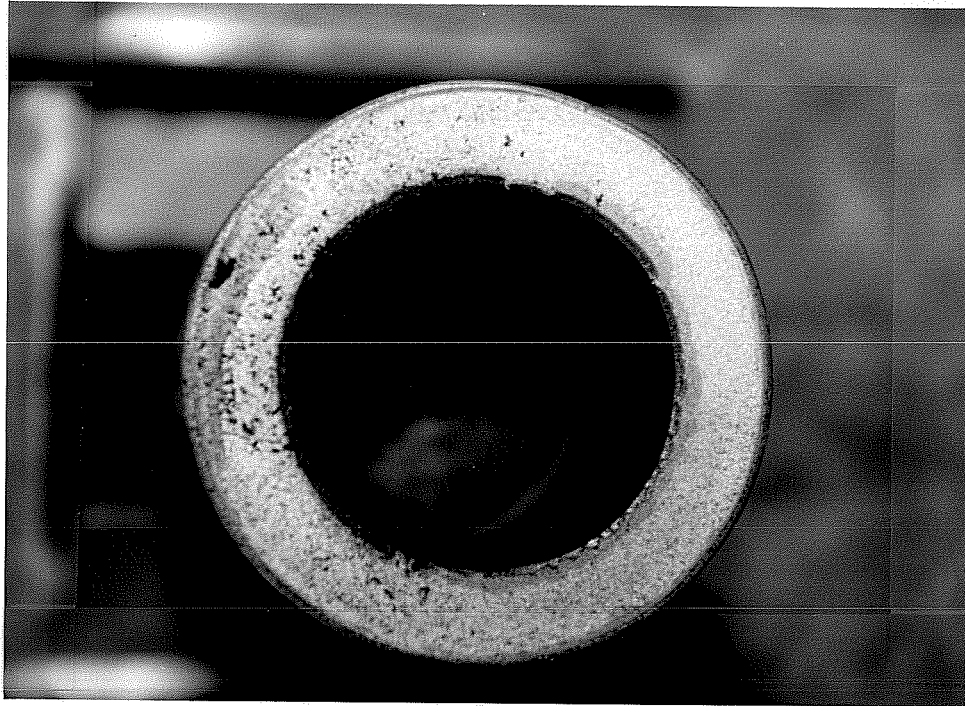


Figure 4.11 Lack of fusion along inner pipe wall.

60° shear wave transducers placed along the wall of the pipe may help in detecting these flaws. Additional testing is required to confirm this point.

4.5 HARDNESS TESTING RESULTS.

4.5.1 MACRO-HARDNESS WELD TESTING RESULTS.

A comprehensive characterization of homopolar weld hardness properties has been carried out. Longitudinal hardness profiles were constructed for welds 2.08, 2.11, 2.21, 2.24, 2.26, 2.27, and 2.29. Readings on these welds' were taken along the pipe's outer wall, along the wall's mid-thickness, and along the pipe's inner wall.

In addition to longitudinal profiles, circumferential hardness surveys were taken on welds 2.08 and 2.11.

Average, highest overall, and lowest overall hardness profiles were constructed from the gathered data. These are shown in Figures 4.12 through 4.14. Average weld hardnesses were obtained by averaging the hardnesses obtained during the testing of the welds mentioned above. Highest overall profiles were obtained by selecting the highest recorded reading at each location along any pipe. The same procedure was used in constructing the lowest overall hardness profiles. Therefore, Figures 4.12 through 4.14 provide bands of expected homopolar weld hardnesses.

AVERAGE WELD HARDNESS PROFILES

OUTER WALL READINGS, (BASE METAL R_b VALUE = 85 R_b)

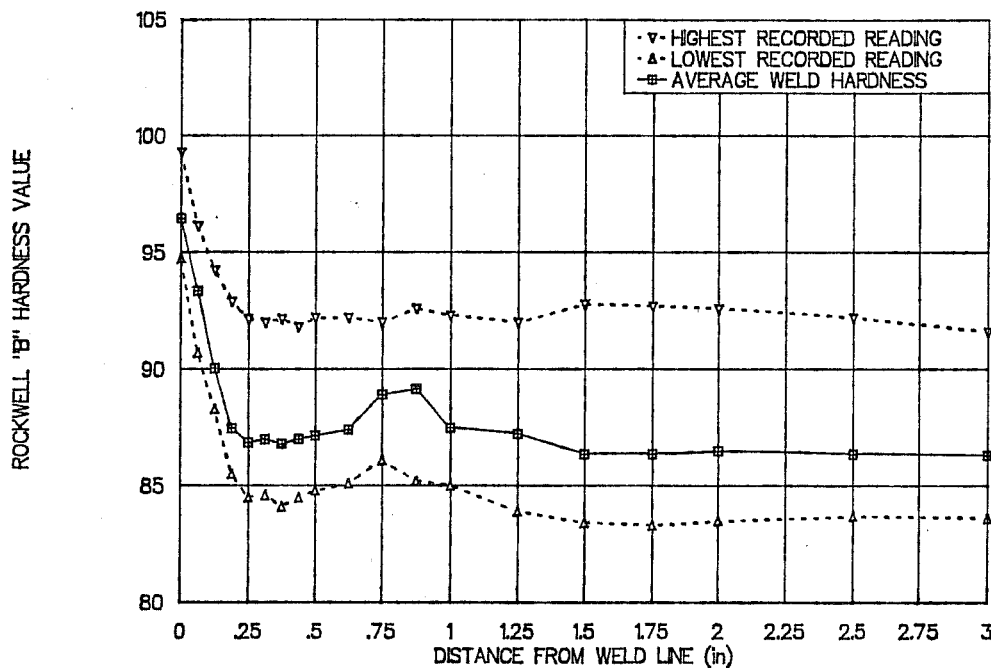


Figure 4.12 Band of expected hardness variation - Outer pipe wall.

AVERAGE WELD HARDNESS PROFILES
MID THICKNESS READINGS. (BASE METAL R_b VALUE = 85 R_b)

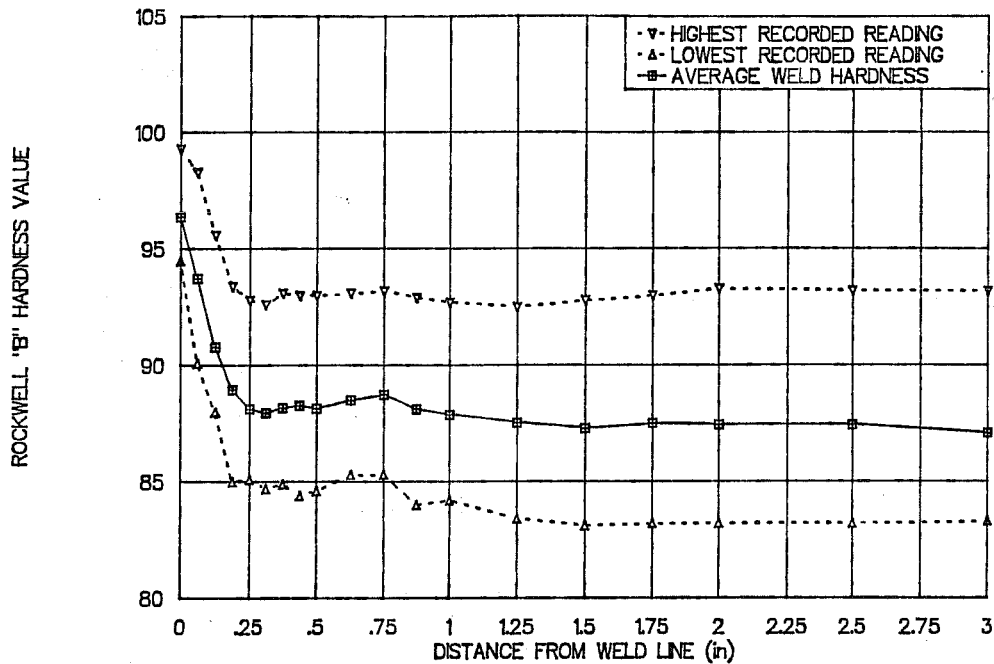


Figure 4.13 Band of expected hardness variation - Mid thickness.

All profiles show a clear difference between weld line and base metal hardness levels. While base metal values average 85 R_b, weld line values average 96 R_b. This differential corresponds to a difference in tensile strength of 35 ksi; the weld zone being stronger than the base metal.

Hardness values begin rising along the electrode contact zone. As shown in Figure 4.15, this region extends between 0.75" and 1.5" away from the weld line. As discussed later, the presence of increased hardnesses along this region agrees with results obtained through specimen etching. The size of the weld's heat affected zone is a function of the distance between the weld line and the electrode contact zone.

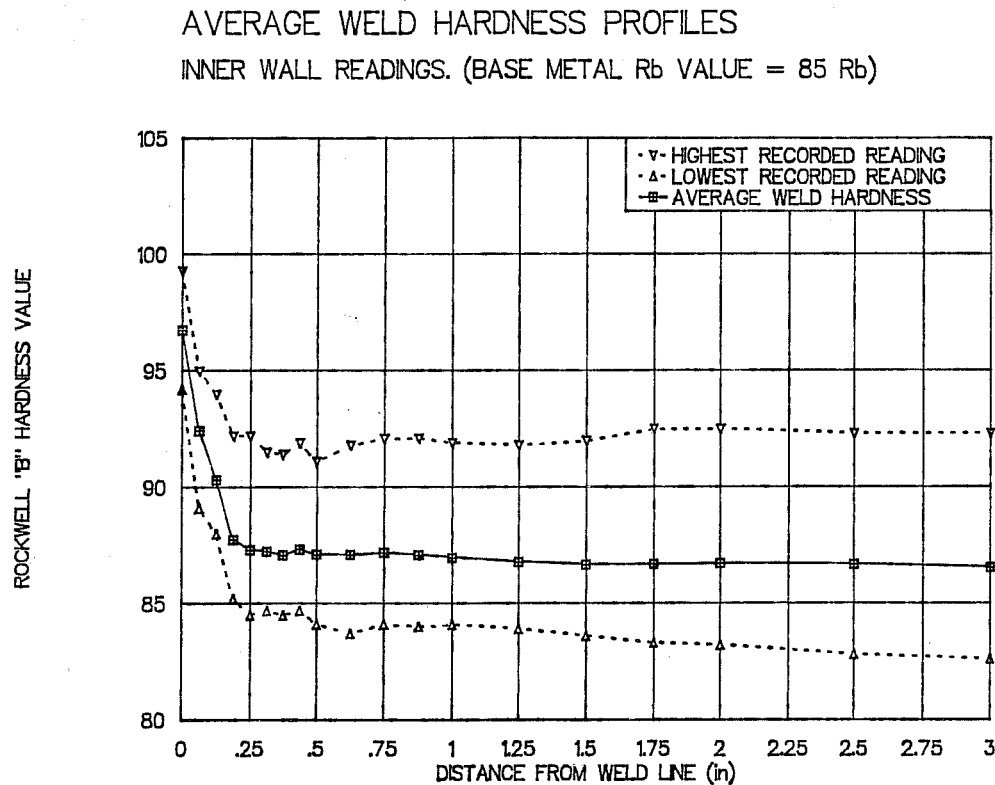


Figure 4.14 Band of expected hardness variation - Inner pipe wall.

Although hardness values begin rising at points of electrical contact, high hardness values are localized along a distance of ± 0.25 " from the weld plane. This confirms that surface resistance is high enough to focus heating at the weld's interface. In addition, lower heat affected zone hardnesses show that this region's cooling rate was slow. As discussed in the next chapter, the possibility of high heat affected zone hardness is eliminated by continued post upset bulk heating.

Peak hardness values are not high enough to indicate the formation of martensite. Hardness values corresponding to martensite are closer to 60 on the Rockwell "C" scale. The highest recorded weld line hardness is 98 R_b. This corresponds to a hardness of 20 on the Rockwell "C" scale.

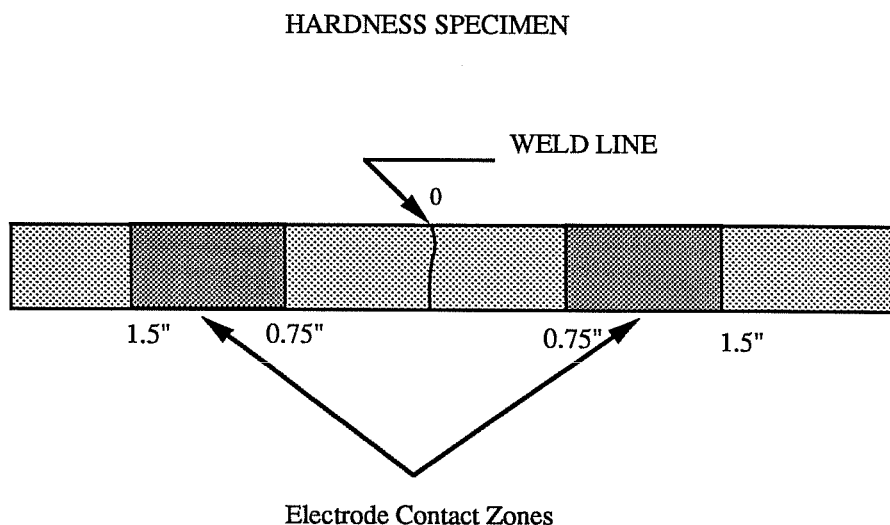


Figure 4.15 Location of electrode contact zones.

It must be kept in mind that all hardness tests were conducted on welds fabricated before the hydraulic overhaul which were all classified as unacceptable welds. As described before, initial pressure drifting in these welds may have resulted in insufficient surface heating. Welds fabricated after the hydraulic modification may be getting hotter since pressure drifting was eliminated. Although higher weld line hardnesses should be expected, the formation of martensitic type hardnesses is unlikely. Bulk heating should continue to prevent fast cooling rates which then promote the formation of high heat affected zone hardnesses. This point will be studied in future research work.

Figure 4.12 confirms the presence of local hard spots along the electrode contact zone. As mentioned in the section on tension results, the fracture of welds 2.31, 2.35, 2.36, 2.40, 2.42, 2.47, and 2.49 seemed to have been initiated by hard spots along the electrode contact zone. The presence of hard spots is confirmed by the hardness hump at points of electrical contact.

Comparing Figures 4.12 through 4.14 reveals that hard spots concentrate along the pipe's outer wall, and do not appear within the wall thickness. This

observation reconfirms that electrode-pipe arcing may be occurring. As mentioned before, local arcing is unacceptable.

Figure 4.16 shows the overall weld hardness range. This figure serves as an indication of maximum and minimum expected homopolar hardness levels. Note that the average hardness profile for weld 2.26 is shown. As shown, hardness values obtained for weld 2.26 constitute the upper portion of the hardness range. It is not known why weld 2.26 developed such high hardnesses. Most welds showed hardness levels lower than those shown by weld 2.26. This point is proven by the overall weld hardness average. Therefore, hardnesses closer to the lower end of the range should be expected.

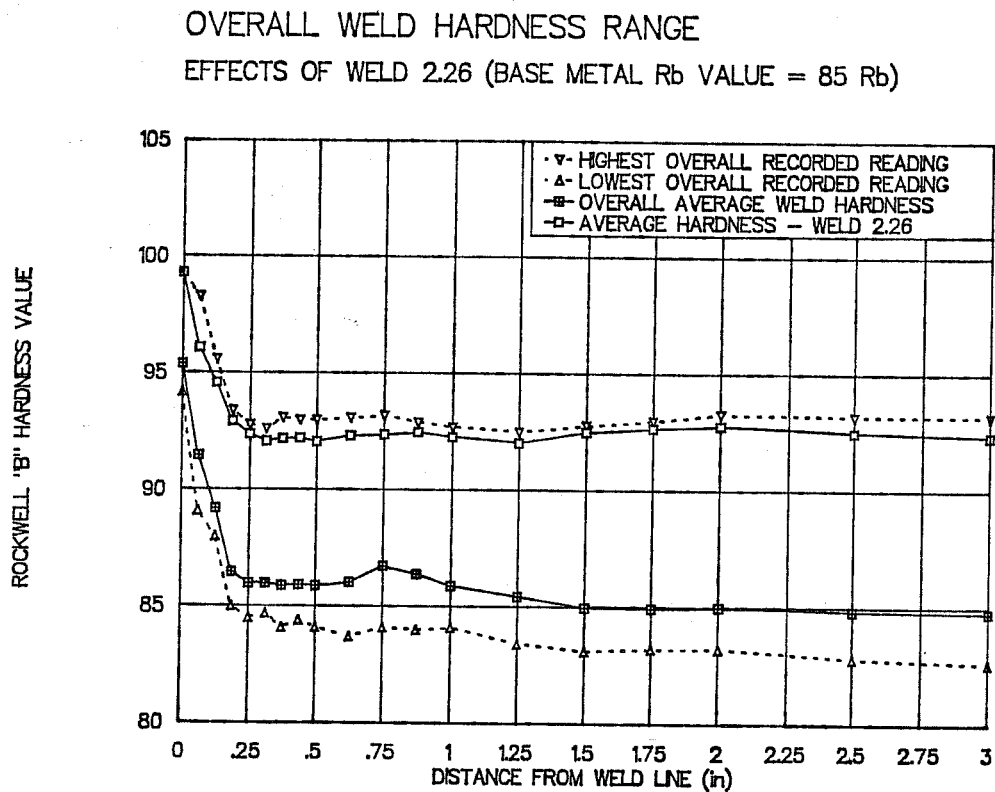


Figure 4.16 Overall homopolar hardness range.

Figure 4.17 shows that the highest average hardnesses formed along the outer pipe wall. This may be attributed to faster cooling rates along this zone. Therefore, only outer wall hardnesses are required for the construction of worst case hardness envelopes. This might become a useful tool for non-destructive weld characterizations and evaluations.

OVERALL WELD HARDNESS AVERAGES
(BASE METAL R_b VALUE = 85 R_b)

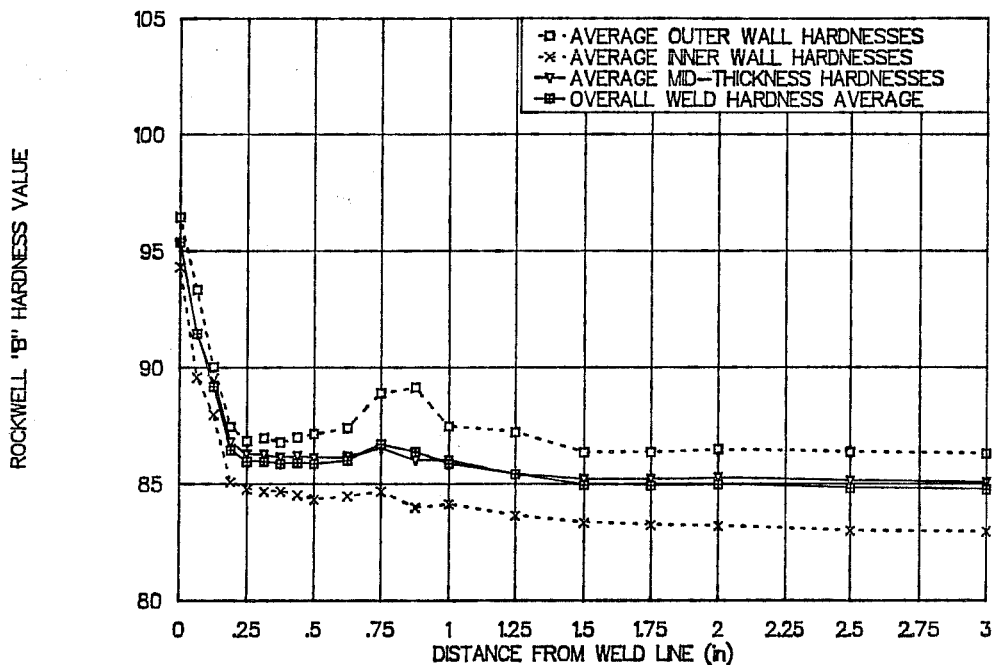


Figure 4.17 Average weld hardnesses.

As shown in Figure 4.18, weld line hardness profiles are fairly uniform. This profiles were constructed from through thickness, weld surface hardness readings taken on weld 2.08. The presence of a uniform through thickness weld line hardness

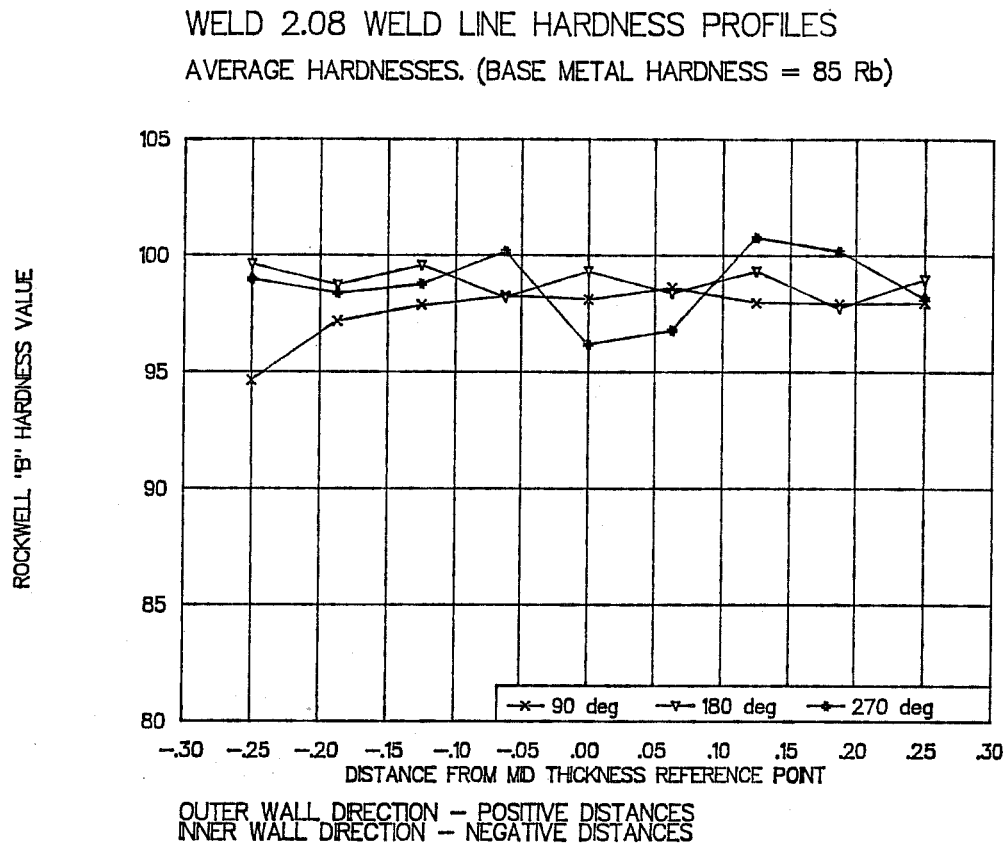


Figure 4.18 Weld line hardness profiles.

profile cannot be used to explain the presence of radial flaws along the inner pipe wall of weld 2.08

In addition to longitudinal hardness testing, welds 2.08 and 2.11 were subjected to circumferential hardness evaluations. As shown in Figure 4.19, hardness specimens were taken from all four pipe quadrants. All hardness testing was done using the Rockwell "B" scale.

Figure 4.20 shows that some circumferential hardness variation was found away from the weld line. This finding agrees with circumferential bonding problems shown by these welds. Although pressure drifting may have contributed, it

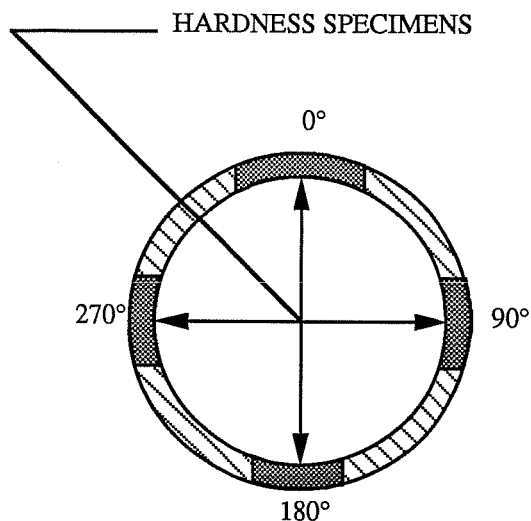


Figure 4.19 Location of hardness specimens - Welds 2.08 and 2.11.

is more likely that improper current distributions through the electrodes, lack of press alignment, or circumferential fixture stiffness variation are causing such variation. Circumferential hardness studies on welds fabricated with the new hydraulic arrangement need to be carried out to determine the exact cause of circumferential hardness variation.

4.5.2 MICRO-HARDNESS WELD TESTING RESULTS.

Knoop micro-hardness readings were taken on weld 2.22. These readings were then compared to Rockwell "B" macro-hardness values obtained from the same weld. A summary of these results is shown in Figure 4.21. Note, all Knoop hardnesses were converted to the Rockwell "B" scale.

Micro-hardness testing has shown higher hardnesses than macro-hardness testing. Knoop values even suggest the formation of martensite within the weld. As

WELD 2.08 CIRCUMFERENTIAL HARDNESS SURVEY
 AVERAGE HARDNESSES. (BASE METAL HARDNESS = 85 Rb)

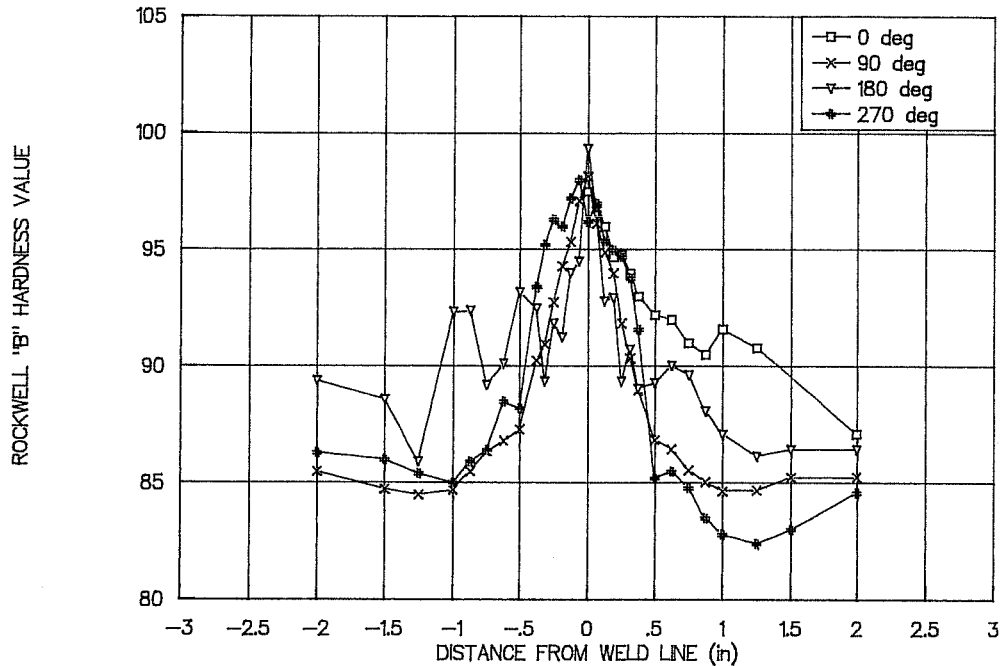


Figure 4.20 Circumferential hardness variation.

mentioned above, extensive macro-hardness testing does not support this point. It is felt that micro-hardness readings are not true indicators of overall weld quality. Micro-hardness points are taken along very local zones. As shown in Figure 4.21, micro-hardness testing extended a distance of only ± 0.35 " away from the weld line. Macro-hardness values were taken up to ± 3.0 " away from the weld line. Thus, the effects of features which do not affect the overall quality of the joint, such as small carbide inclusions, are over emphasized through micro-hardness testing. Therefore, it is not felt that these micro-hardness readings are of much consequence.

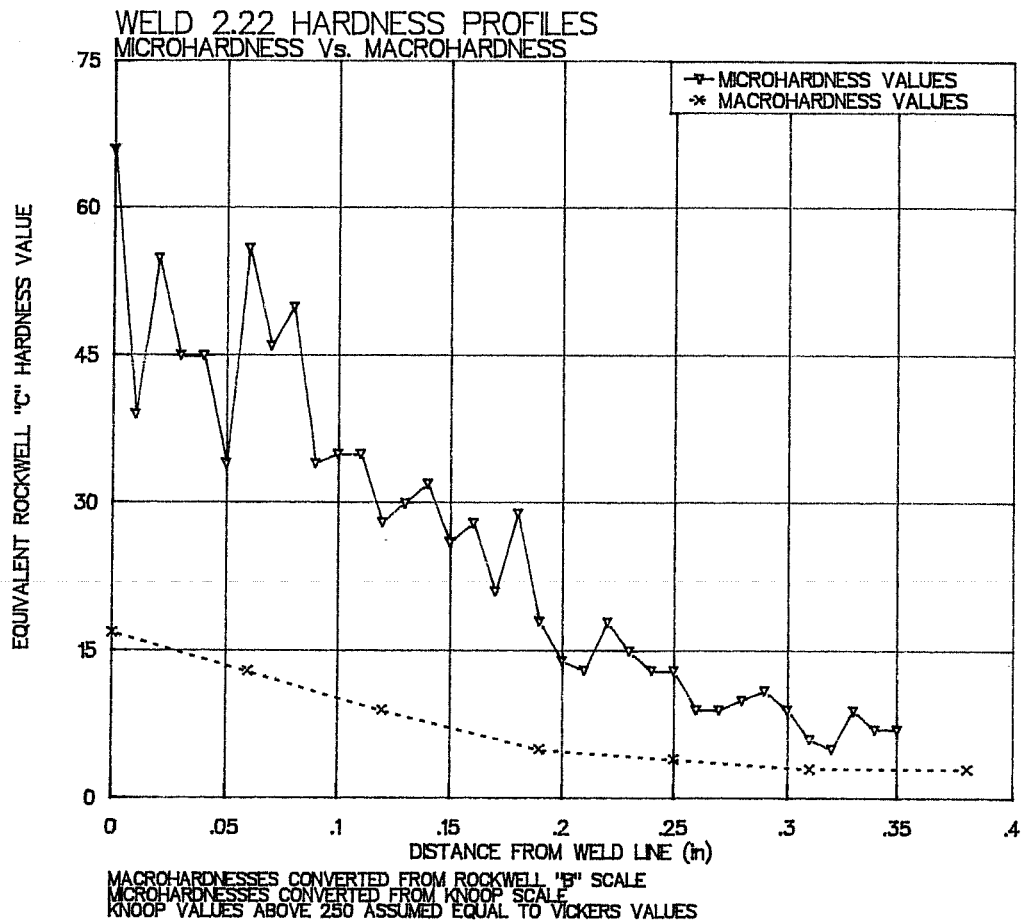


Figure 4.21 Micro-hardness and macro-hardness results - Weld 2.22.

4.6 CHARPY V-NOTCH TESTING RESULTS.

Weld 2.08 was subjected to Charpy V-notch testing. Toughness values were obtained for the weld line and the heat affected zone. These were then compared to base metal values. Toughness results plotted in Figure 4.22 show that severe

WELD 2.08 — CHARPY V-NOTCH VALUES
WELD LINE AND HEAT AFFECTED ZONE TOUGHNESSES

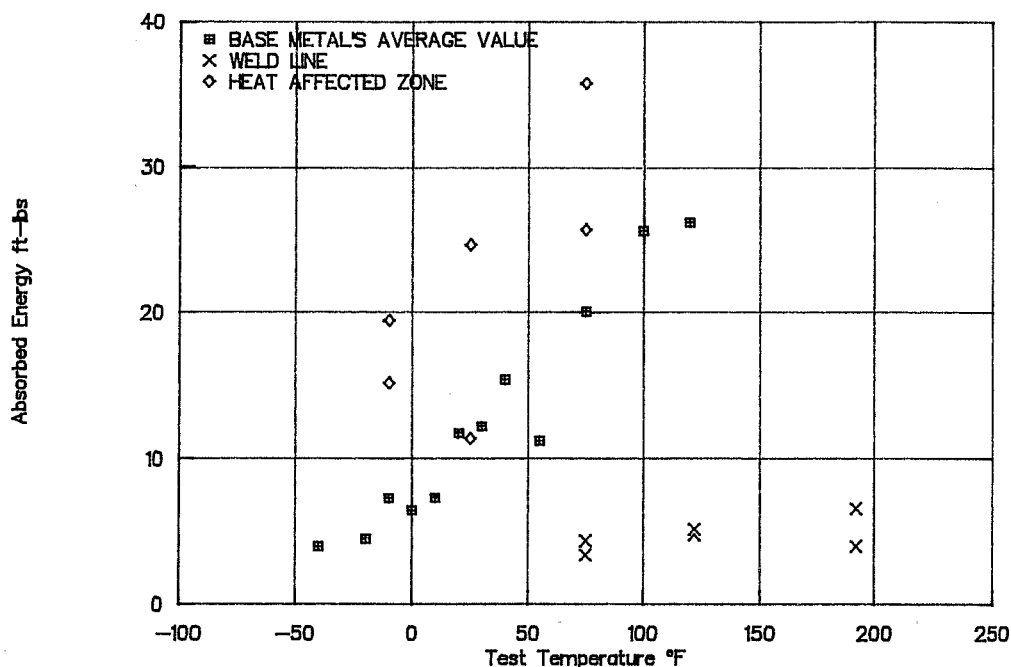


Figure 4.22 Homopolar toughness performance - Weld 2.08.

loss of toughness was experienced along the weld surface. Such loss of toughness is unacceptable if homopolar welding is to be incorporated for offshore pipeline work.

Figure 4.22 also shows that heat affected zone toughness values are equal to, or higher than, the base metal toughness. Heat affected zone specimens were notched 1/16" away from the weld line. Therefore, loss of toughness is localized along the weld surface. This result reconfirms that the quality of a homopolar weld is mainly dependant on the quality of the weld plane, and not on the heat affected zone. It is clear that slow cooling rates, produced by high bulk heating, have prevented the degradation of heat affected zone properties.

It is very important that Charpy testing be continued. Charpy testing has not been done on either heat treated specimens or on welds made after the hydraulic overhaul. As mentioned before, the elimination of initial pressure drifting has resulted in higher interface heating. The effects of higher weld temperatures must now be assessed in terms of weld toughness. Heat treated welds need to be tested to determine whether or not weld line toughnesses are regained through post-weld heat treatment. Added to this, a larger toughness data base needs to be established since only one weld has been tested.

4.7 ETCHING RESULTS.

Both hardness and Charpy v-notch specimens were lightly etched before being tested. Etched samples confirmed that microstructural changes were produced by the weld's thermal cycle. These changes extend between the weld line and the electrode contact zone. Figure 4.23 shows a set of typical etch patterns.

The most significant characteristic revealed through etching is the presence of a well defined weld plane. Its presence raises questions concerning the homopolar bonding process. It is not known whether localized melting along the joint's surface, whether atomic diffusion, or whether other forging processes lead to a welded joint. Whatever the bonding process is, tensile, Charpy v-notch, and hardness results show that the quality of this weld plane is the main factor affecting the performance of the joints.

As shown in Figure 4.23, microstructural changes are not localized along the weld plane. These changes extend up to the electrode contact zone. Heating caused by simple material resistivity is high enough to produce microstructural changes away from the weld line. Thus, the size of the heat affected zone is clearly a function of the material's resistivity, of the weld energy input, and of the distance between electrode contact and joint interface.

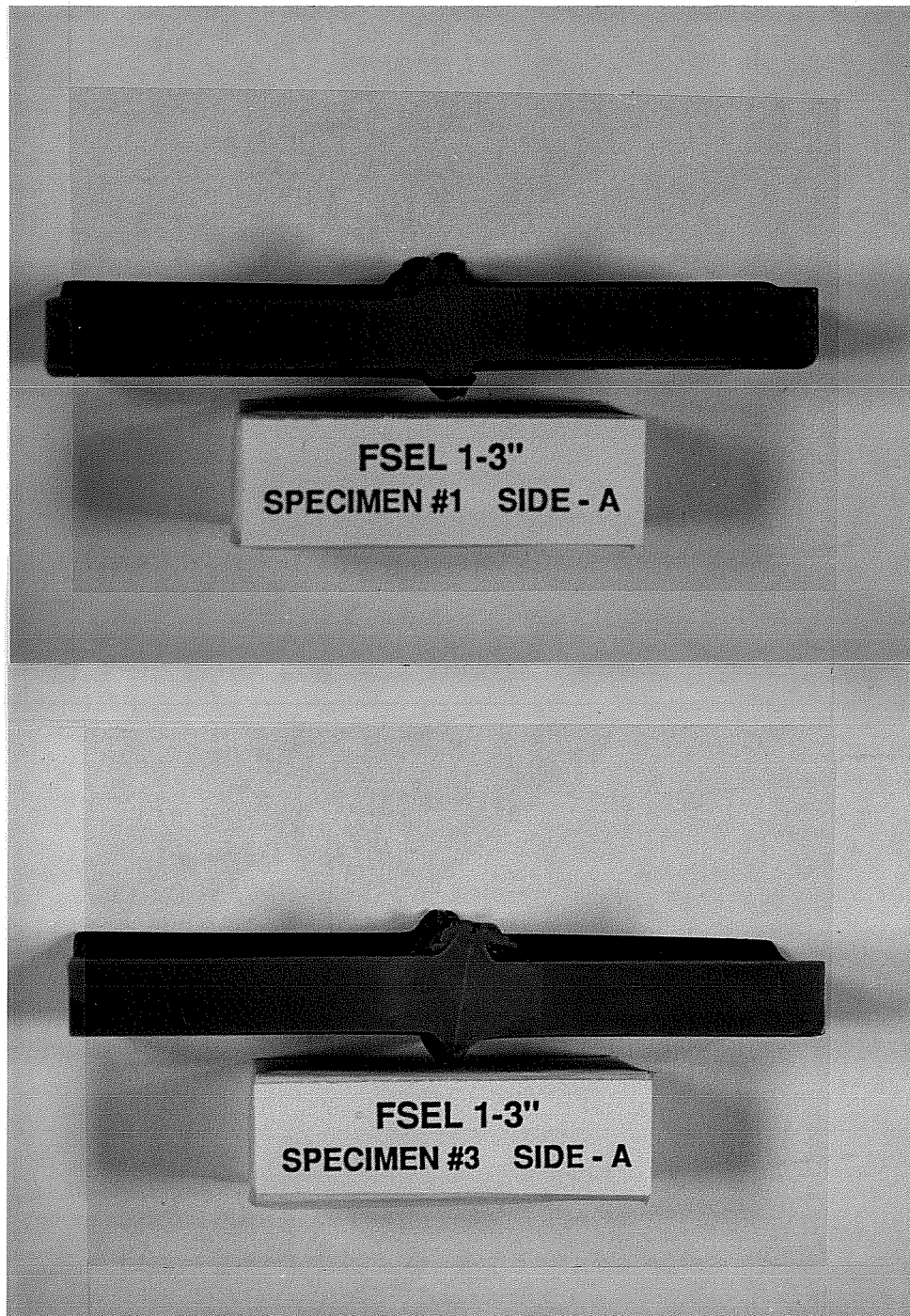


Figure 4.23 Typical etch patterns.

4.8 MICROSTRUCTURAL ANALYSIS.

A microstructural characterization of the base metal, weld planes, and heat affected zones was completed. This analysis has shown the presence of acicular ferrite along the weld plane, and grain refinement along the heat affected zone. A full discussion on this topic is presented in the next chapter. There, these properties are used to explain the characteristics and consequences of the homopolar thermal cycle.

4.9 SURFACE RESISTANCE TESTING.

The effects of end preparation on surface resistance have been studied. Seven surface conditions were tested to determine which end preparation provides the best surface resistance for homopolar pulse welding. Surface resistance, thus heat generation, is a direct function of end preparation. The quality of end preparations is measured by its reproducibility, by its heat generation capacity, and by how well it distributes current across the weld surface. Tested surfaces breakdown as follows: a rough band saw cut, three rough machined finishes, and three filler wire meshes.(13). Resistances were measured using a microOhm meter.

A rough band saw cut finish produces the highest surface resistance. Unfortunately, control over this surface finish is minimal. Since natural irregularities within a band saw cut finish affect the distribution of current within the joint surface, weld reproducibility may be sacrificed if this surface is used.(13). Machined preparations produce less surface resistance than a band saw. However, these surfaces are fully controlled; thus eliminating some of the questions concerning weld reproducibility. Wire screens produce surface resistances that are comparable to those produced by a rough band saw cut.(13). Added to this, meshes provide a controlled surface finish which produces a more uniform current distribution across the joint surface. Meshes, however, introduce a new set of problems. Problems such as void formation and extrusion of the mesh material need to be studied.

There is a need for continued research in the area of surface preparation. Although preliminary conclusions have been made, the amount of data is still limited.

4.10 WELD TEMPERATURE MEASUREMENTS.

As mentioned in the section above, more work is needed to understand the factors affecting current distribution and surface heating. One particular area that must be investigated is the measurement of joint temperatures. Very few temperature measurements have been carried out to date. Only a limited amount of data has been gathered through the use of temperature paints.

Before this investigation started, bonding was believed to occur through forging at temperatures close to 800°C. Temperature measurements do not confirm this. Temperatures reaching 1350°C at 0.25 inches away from the weld line were measured. Continued temperature testing is planned. Thermocouples and temperature paints will be placed in future welds.

4.11 EFFECTS OF POST WELD HEAT TREATMENT.

The effects of post weld heat treatment on homopolar weld quality have been studied. Several weld samples were subjected to different levels of post-heat treatment and then tested.

One specimen was heated at 1500°C for ten minutes and then air cooled. 1500°C is well within the material's austenizing range. This specimen was then subjected to Rockwell "B" hardness testing.

Figure 4.24 shows the results of the 1500°C heat treatment. Two hardness profiles are shown on Figure 4.24; one profile showing as welded hardnesses, the other showing heat treated hardnesses. It is clear that base metal hardnesses are regained through the application of post weld heat treatment.

Additional testing was done using lower heat treatment temperatures. Two specimens were heat treated for fifteen minutes at 900°C, 1100°C. Hardness levels in these specimens remained high. Both specimens continued to show weldline hardnesses close to 98 Rb, as compared to the base metal's 85 Rb. Weld normalization has only been achieved by applying a 1500°C heat treatment for ten minutes. Additional testing is required to determine a minimum heat treatment temperature.

The successfully heat treated specimen was then etched. Etching this sample revealed that microstructural changes were in fact eliminated through the

WELD 2.21 HARDNESS PROFILES

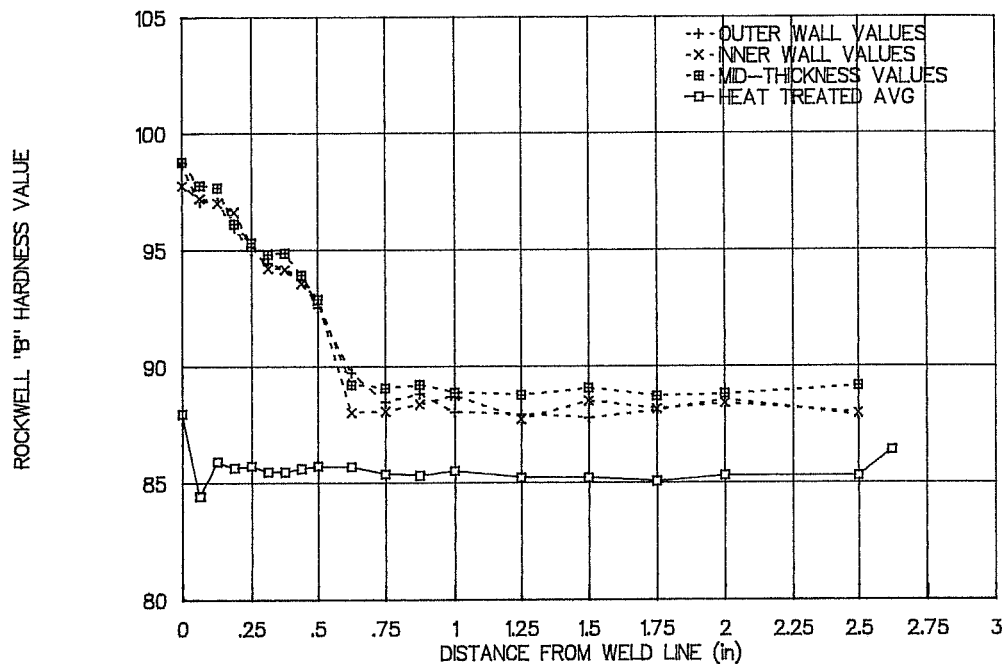
AVERAGE HARDNESS READINGS. (BASE METAL R_b VALUE = 85 R_b)

Figure 4.24 Effects of post-weld heat treatment on weld hardness.

application of the 1500°C post-weld heat treatment, thus agreeing with post-weld heat treatment hardness results.

The effects of post-weld heat treatment on weld toughness have not been studied. As mentioned before, severe loss of toughness has been experienced along the weld plane. Base metal toughnesses must be regained if homopolar pulse welding is to be accepted by industry. Efforts are being planned for the testing of normalized charpy specimens.

4.12 SIGNIFICANCE OF RESULTS.

The development of this chapter constitutes the result of initial efforts in the investigation of homopolar pulse welding. Data reported in this chapter now serves as a guide for continued research.

One of the biggest questions concerning homopolar pulse welding is the lack of weld reproducibility. No consistent reason has been formed to explain why welds fabricated using the same set of welding parameters have produced very different test results.

Although improvements have been made through the incorporation of the closed loop servo-controlled hydraulic system, it is not known whether lack of weld reproducibility has been fully eliminated. Other factors, such as lack of axial alignment, fixture stiffness variation, and surface current variation, may also be contributing to weld variability.

A better understanding of the surface heating process needs to be developed. As mentioned in the section on tension results, peripheral flaws were found along the inner wall of several tested specimens. These flaws suggest that heating starts along the outer wall region, and gradually moves into the inner wall region. A clear picture of the nature of this thermal process needs to be developed in order to avoid the formation of such defects. In addition, studies using ramped upset pressures need to be done. Using ramp pressure functions, as opposed to step functions, may result in higher and more prolonged interface heating. As mentioned in chapter three, the incorporation of a function generator into the hydraulic system makes these studies possible.

Continued research is required in the area of surface preparation. Surface conditions have a significant effect on the overall current distribution. The use of better controlled surfaces may help in eliminating the formation of flaws, as well as increasing weld reproducibility.

Temperature investigations need to be continued. Measurements have shown temperatures higher than what was anticipated before this investigation started. Before this investigation started bonding was believed to occur at 800°C; 1350°C temperatures have already been recorded.

Hardness results are very significant. A considerable difference in hardness exists between the base metal and the weld line. Peak weld line hardnesses are not high enough to suggest the formation of martensite. In addition, base metal hardness levels are regained through the use of heat treatment.

Several problems were found through this initial phase of testing. First, severe loss of toughness was experienced along the weld plane. This must be eliminated if homopolar welding is to be used for pipeline construction. It is felt, however, that some improvements may be obtained through the application of post-weld heat treatment. Because of this, testing of normalized charpy specimens has now become a priority. Second, local hard spots are forming along points of electrical contact. It is possible that local arcing is the cause. If this is happening, it should be eliminated. As with low weld line toughnesses, it is felt that hard spots may be eliminated through post weld heat treatment. Third, copper inclusions have been found along the outer pipe wall of several weld samples. The presence of these inclusions must be eliminated through the use of steel shims.

Ultrasonic techniques seem to be a viable method for weld evaluation. Further testing is required to fully establish its applicability. This testing should include the use of both 45° and 60° compression wave transducers.

Parametric investigations have not been carried out due to the unexpected presence of weld variability. These investigations need to be carried out once weld reproducibility is fully established. To date, most of the welds have been fabricated using weld parameters determined through past experience, or through trial and error. A more rational parameter selection process needs to be developed if industry is to be attracted to homopolar welding.

Finally, only 3.5" x 0.43" pipe has been welded. Different size pipes need to be welded to determine whether or not weld parameters can easily be scaled up or down.

It must be noted, to the credit of homopolar pulse welding, that testing was done using pipe material that is not truly representative of commonly used pipeline material. This material would not be accepted by industry due to the high carbon content. Having welded this steel is very encouraging. The welding of lower carbon steels should be easier. Efforts are being planned to prove this point.

CHAPTER 5

HOMOPOLAR, FLASH-BUTT, FUSION WELD COMPARISON.

The development of J-laying is coupled with the development of an efficient, and reliable automatic welding system. Although significant research is still required, it is felt that homopolar welding is a strong contender for J-lay applications. To prove the applicability of homopolar welding as a viable alternative for pipeline construction, this chapter presents a comparison between homopolar pulsed, flash-butt, and fusion welds. These processes are compared and contrasted in terms of their thermal cycles, weld hardness, weld toughness, and weld production rates.

The chapter begins with a description of the homopolar thermal cycle. This is then followed by brief discussions on the heating cycles of both flash-butt and fusion welds. Weld hardness and weld toughness properties are compared within these discussions. Finally, a comparison of weld turn over rates is given at the end of this chapter.

All flash-butt weld properties presented in this chapter were obtained from literature published by McDermott Inc. McDermott is a leader in the application of flash-butt welding for pipeline construction.

5.1 COMPARISON OF THE WELDS' THERMAL PROCESSES.

5.1.1 HOMOPOLAR THERMAL CYCLE.

Homopolar welding is a high temperature, slow cooling rate welding process. Its thermal cycle is composed of three distinct phases; heat generation before the application of upset load, bulk heating after upset, and weld zone cooling. Although discussed separately, the completion of the thermal cycle takes only a few seconds.

The first phase begins with the discharge of the homopolar generator. Current begins to flow from the generator, through the bus bars, through the electrodes, and finally through the pipes. Two forms of heating quickly occur. Bulk heating is

produced by the material's resistivity; surface heating is produced by the constriction of current along areas of electrical contact. Since surface resistance is much higher than material resistivity, heating is mostly focused along the joint's interface.

Figure 5.1 shows heating during the first thermal phase. Note how heat generation is concentrated at the joint's interface.



Figure 5.1 Interface heating during first homopolar thermal phase.



Figure 5.2 Bulk heating during second homopolar thermal phase.

The second thermal phase begins with the application of upset load. Since most or all interface surface resistance is eliminated during upset, only bulk heating is produced after upset. This is shown in Figure 5.2.

The presence of bulk heating after upset leads to high heat affected zone temperatures. These temperatures reach levels comparable to those seen by the weld plane. As mentioned in chapter four, temperatures close to 1300°C were measured at 0.25 inches away from the weld line.

Pipe cooling begins with the completion of discharge. Due to the presence of bulk heating before and after upset, slow cooling rates are experienced. Figure 5.3 shows a weld during the cooling stage.



Figure 5.3 Weld cooling during third homopolar thermal phase.

The duration of each thermal phase is obtained by looking at the weld's recorded parameter traces. Figure 5.4 shows the voltage, current, and pressure traces for weld 2.22. As shown, discharge occurred at 0.47 secs. Discharge is signaled by sudden surges in both current and voltage. Upset loading was applied at 0.97 secs. Discharge ended at 3.5 secs.

By referring to Figure 5.4 it is known that interface heating took place between discharge at 0.47 secs, and the application of upset pressure at 0.97 secs. Post upset bulk heating occurred between the application of upset load at 0.97 secs, and the end of discharge at 3.5 secs. Cooling started after the completion of discharge.

BEHAVIOR OF WELD PARAMETERS WELD 2.22

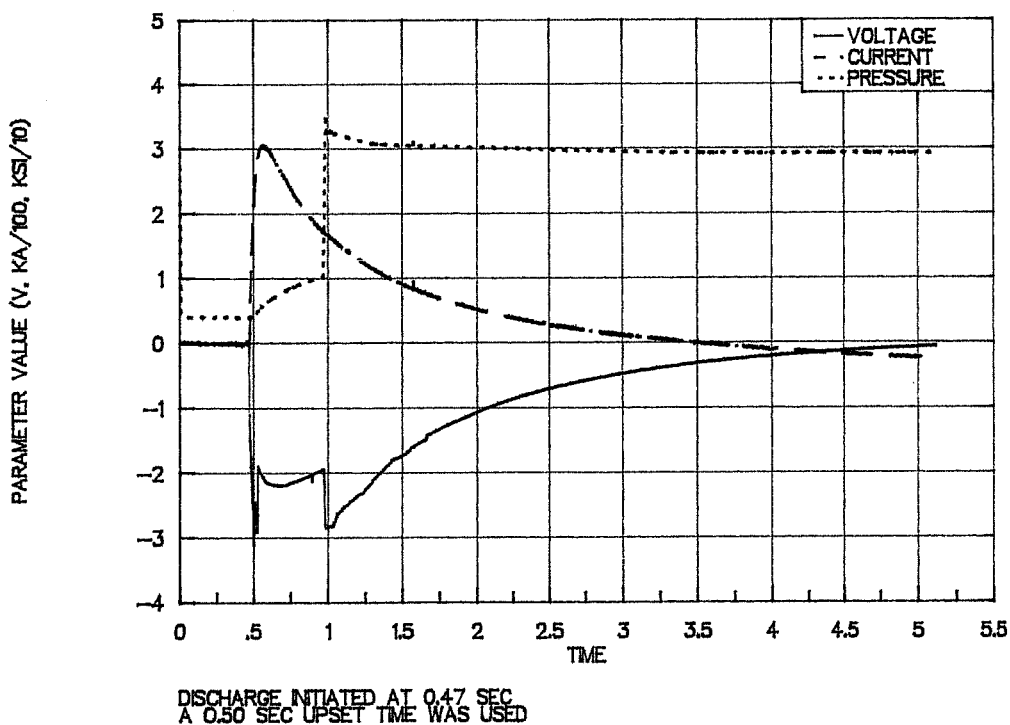


Figure 5.4 Recorded parameter traces - weld 2.22.

Figure 5.5 shows the cumulative energy distribution for weld 2.22. Most of the process' energy was spent in bulk heating after upset. Upset occurred at 0.97 secs. Due to this continued heating, the possibility of experiencing fast heat affected zone cooling rates is eliminated. This then eliminated the presence of either toughness degradation or high hardness formation along the heat affected zone. This point is confirmed by tension and hardness results presented in chapter four.

Studying the microstructures of homopolar welds reveals that the weld's thermal process led to the formation of both acicular ferrite along the weld plane, and grain refinement along the heat affected zone. Figures 5.6, 5.7 and 5.8, show

WELD ENERGY TRACE

WELD 2.22

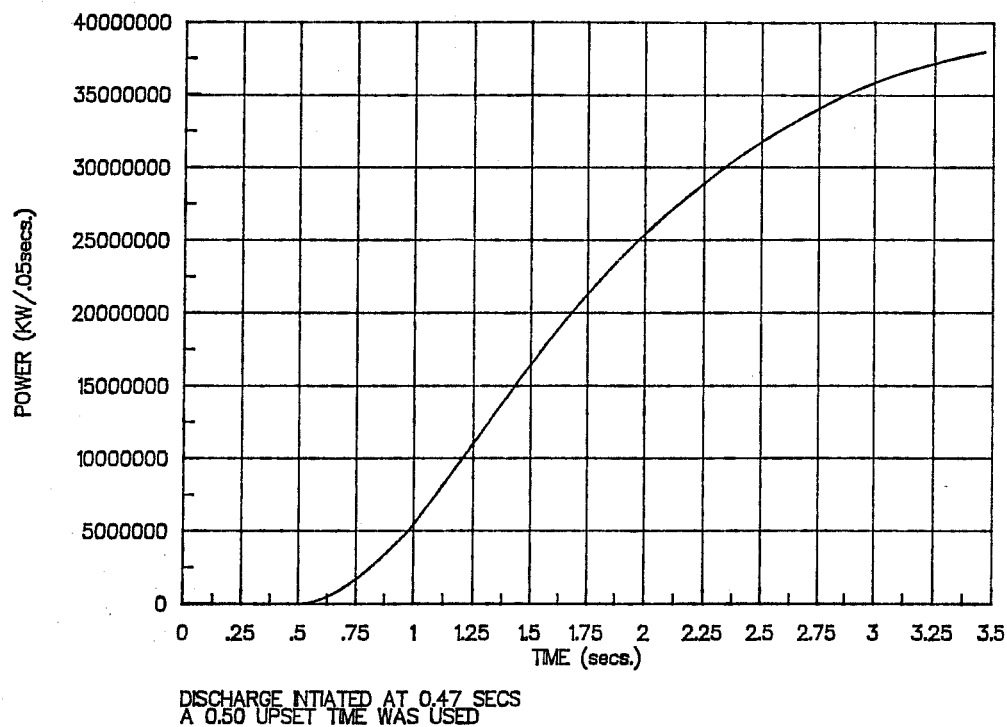


Figure 5.5 Cumulative energy trace - weld 2.22.

micrographs corresponding to the base metal, weld plane, and heat affected zone. Note, these micrographs were taken at both 100X and 400X magnifications.

Figure 5.6 shows the base metal's microstructure. This microstructure is indicative of normalized AISI 1030 steel.(14)

Figure 5.7 shows the weld line microstructure. Again, this microstructure was identified as acicular ferrite. The presence of acicular ferrite confirms that the weld plane reached temperatures well within the steel's austenizing range. The presence of acicular ferrite is also indicative of fast cooling rates. As defined by the ASM Metals Reference Book, "acicular ferrite forms upon continuous cooling by

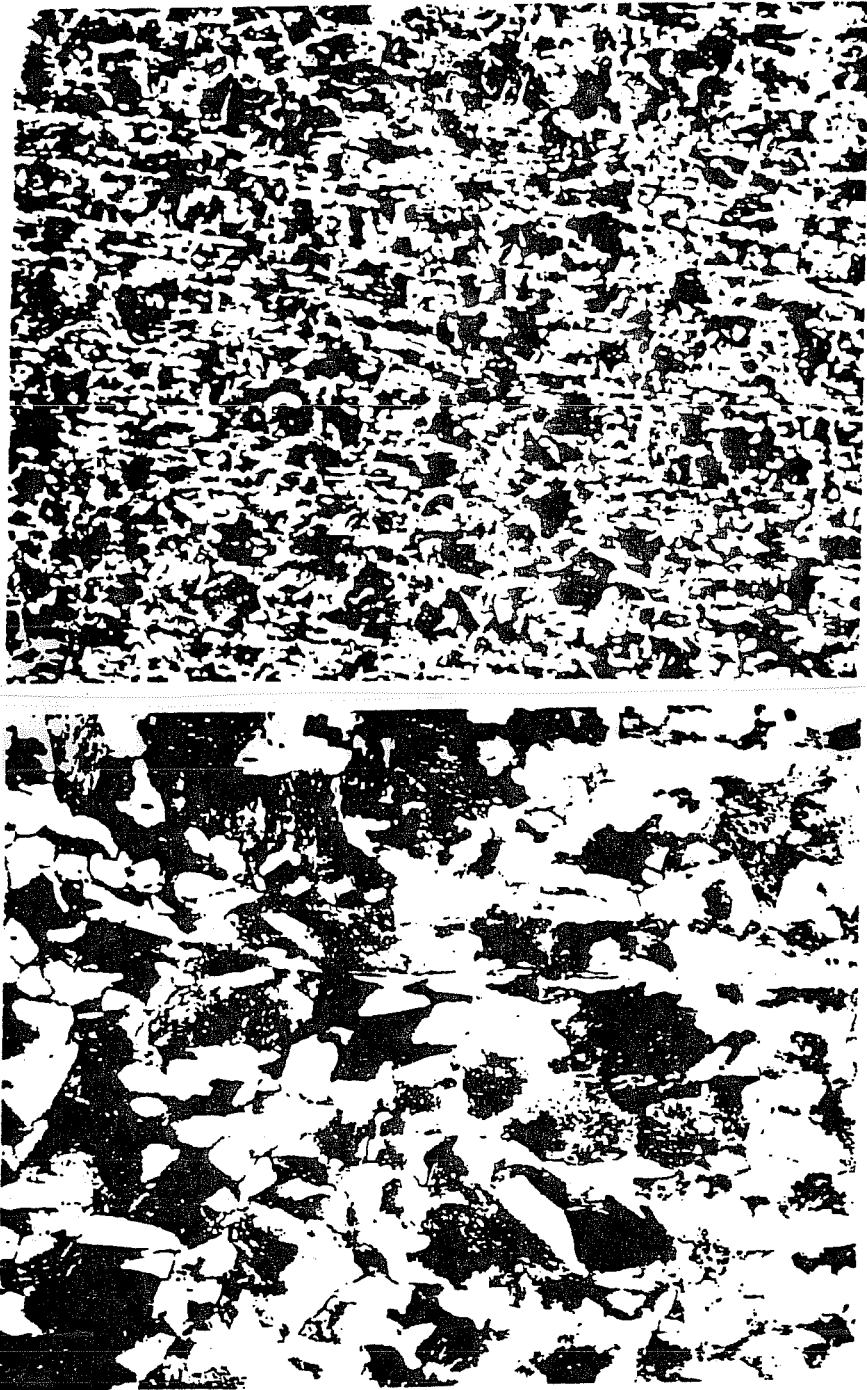


Figure 5.6 Base metal micrographs. 100X and 400X magnifications.(14).

a mixed diffusion and shear mode of transformation that begins at a temperature slightly higher than the temperature transformation range for upper bainite. It is distinguished from bainite in that it has a limited amount of carbon available.”(15). As mentioned above, interface heating disappears as upset load is applied. As this occurs, heat generation is transferred from the weld plane to the surrounding heat affected zone. Weld line quenching may be occurring during this heat transfer process.

As mentioned in chapter four, high hardnesses and loss of toughness were experienced along the weld line. This degradation of weld line properties is explained by the presence of acicular ferrite, and by the fast cooling rate associated with it.

Figure 5.8 shows the heat affected zone microstructure. It is clear, by comparing with Figure 5.7, that grain refinement occurred. Therefore, the heat affected zone also reached temperatures within the austenizing range. In addition, grain refinement shows that cooling was slow enough to avoid the formation of acicular ferrite, but fast enough to avoid grain coarsening.

The presence of a grain refinement indicates that homopolar welding produces acceptable quality heat affected zones even when welding high carbon steels. However, problems may occur when welding stainless steel. Stainless steel is susceptible to softening produced by grain refinement.

5.1.2 FLASH-BUTT THERMAL CYCLE.

Homopolar and flash-butt welding are very similar in nature. Both constitute fully automated solid state resistance/forging welding systems. By definition, both processes rely on interface surface resistance for heat generation. In addition, both use an applied upset load for joint forging. By being resistance/forging welding processes, both methods offer rapid one station welding, therefore making them attractive alternatives for J-lay applications.

Like homopolar welding, flash-butt welding relative to fusion welding is a low temperature, slow cooling rate welding process. Added to this, its thermal process can also be broken down into three parts; initial heat generation, increase of joint thermal gradient before upset, and weld cooling after upset. Flash-butt welding

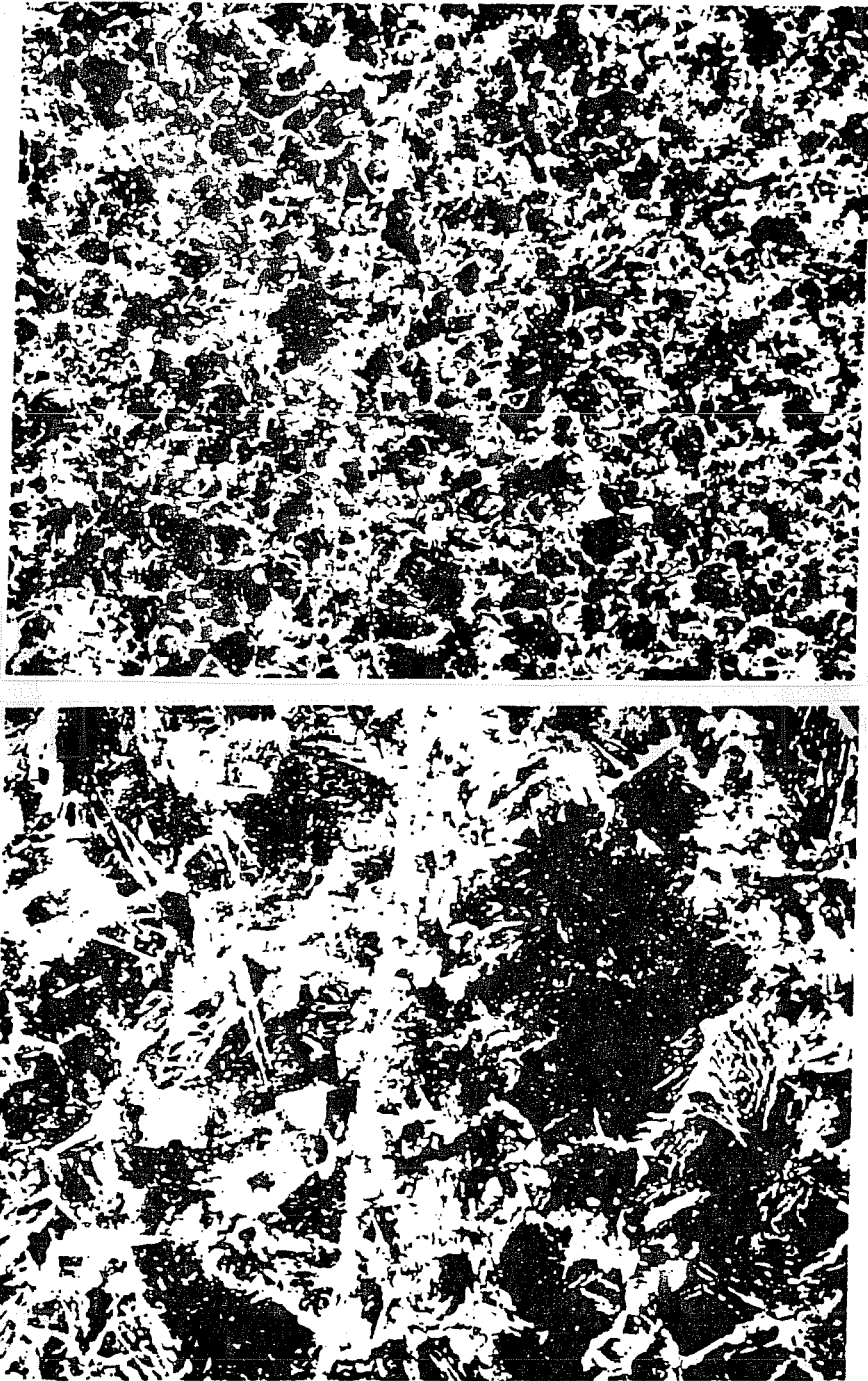


Figure 5.7 Weld plane micrographs. 100X and 400X magnifications.(14).

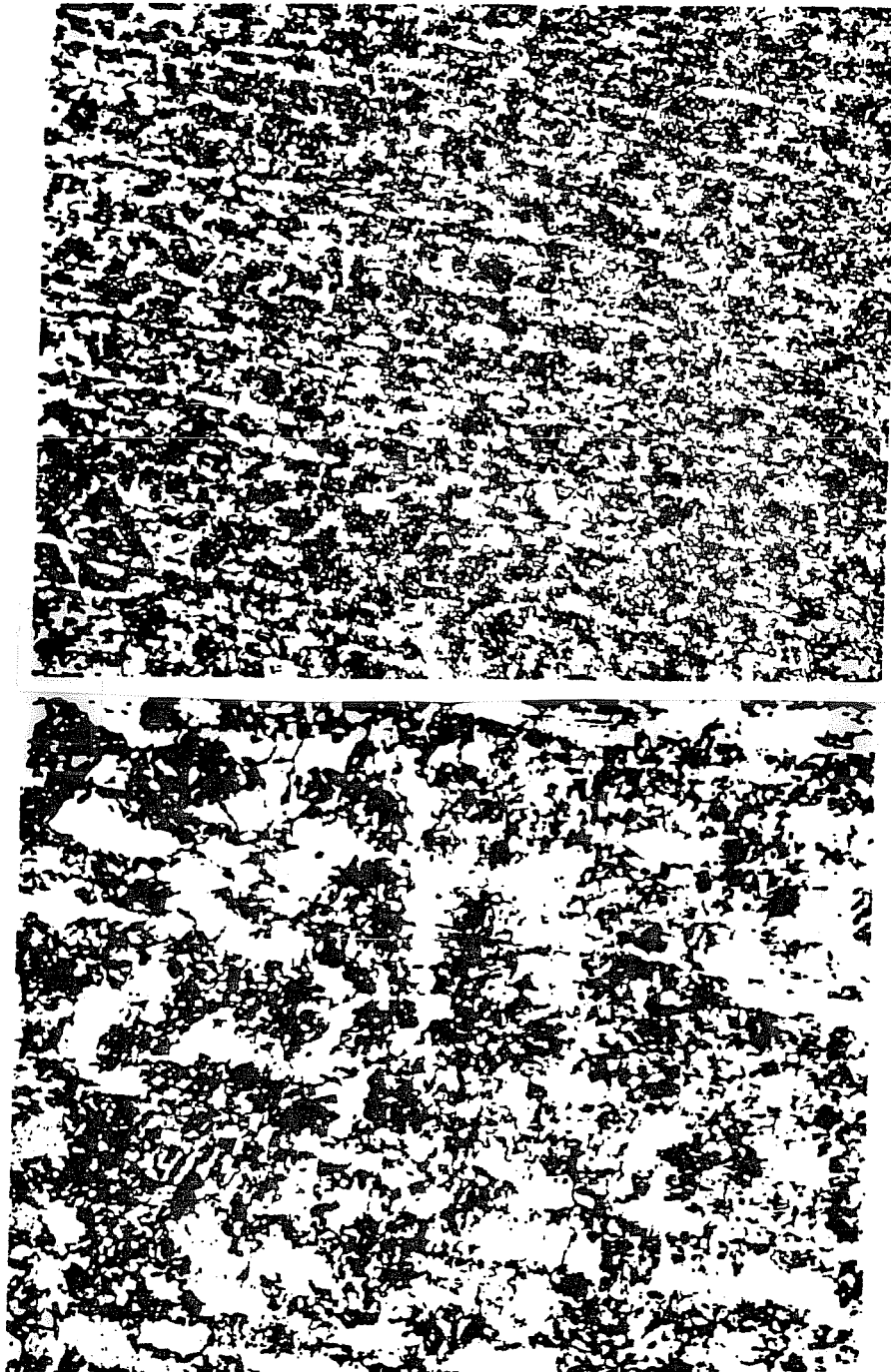


Figure 5.8 Heat affected zone micrographs. 100X and 400X magnifications.(14).

begins with the application of low voltage, high ampere current to the pipes. This is done while slowly moving the pipes together. Like homopolar welding, bulk resistive heating and joint surface heating are generated as electrical contact is made between pipes.

As the pipes become red hot, the weld's thermal gradient is raised by increasing the speed at which the pipes' are being brought together. Heat concentration at the joint's interface is required to complete a flash-butt weld. Faster axial speeds result in higher interface conductive heating and weld flashing.

High interface heating is allowed to continue for about half a minute. At the end of this time, the pipe ends are white hot. The white hot pipes are then quickly forged together. At this point in time the joint is completed, and the pipes are allowed to cool.

The biggest differences between flash-butt and homopolar welding lie within the nature and duration of the welds' thermal cycles. First, heating of flash-butt welds is slower and higher than heating of homopolar welds. Because of this, flash-butt welds spend longer lengths of time at an austenizing temperature; thus making flash-butt welding more susceptible to grain growth. Common flash-butt welding practices require the application of post weld heat treatment for the elimination of coarsened structures. Second, while most of the homopolar's weld energy is used for bulk heating after pipe forging, flash-butt welding uses most of its energy on interface heat generation. This produces a well defined thermal gradient which is not seen in homopolar welds. This gradient causes flash-butt welds to experience faster cooling rates than homopolar welds. Because of this, flash-butt welds show broader, lower quality heat affected zones than homopolar welds.

The relative effects on weld quality produced by the homopolar and the flash-butt thermal cycles are established through the study of weld hardnesses and weld toughnesses.

Figure 5.9 shows hardness profiles obtained for both flash- butt and homopolar pulse welds. Flash-butt hardness values were obtained from reference 7. These readings were taken on API 5LX Grade 65 pipe welds. Section 3, "Chemical Properties and Tests", of API 5L specifications for line pipe limits the maximum

carbon content of this steel to 0.26%. Flash-butt readings had to be converted from the Vickers scale to the Rockwell "B" scale.

Homopolar values constitute averages of the hardness data presented in chapter 4. Again, 0.36% carbon steel was used in the homopolar research program. This steel has a higher hardenability than API 5LX Grade 65 steel.

As shown in Figure 5.9, even with the higher carbon content, homopolar welds showed similar, or even lower peak hardnesses than flash-butt welds. Added to this, heat affected zone hardnesses were higher in flash-butt welds than in homopolar welds. This agrees with the differences in the thermal cycle of the two welding processes presented above.

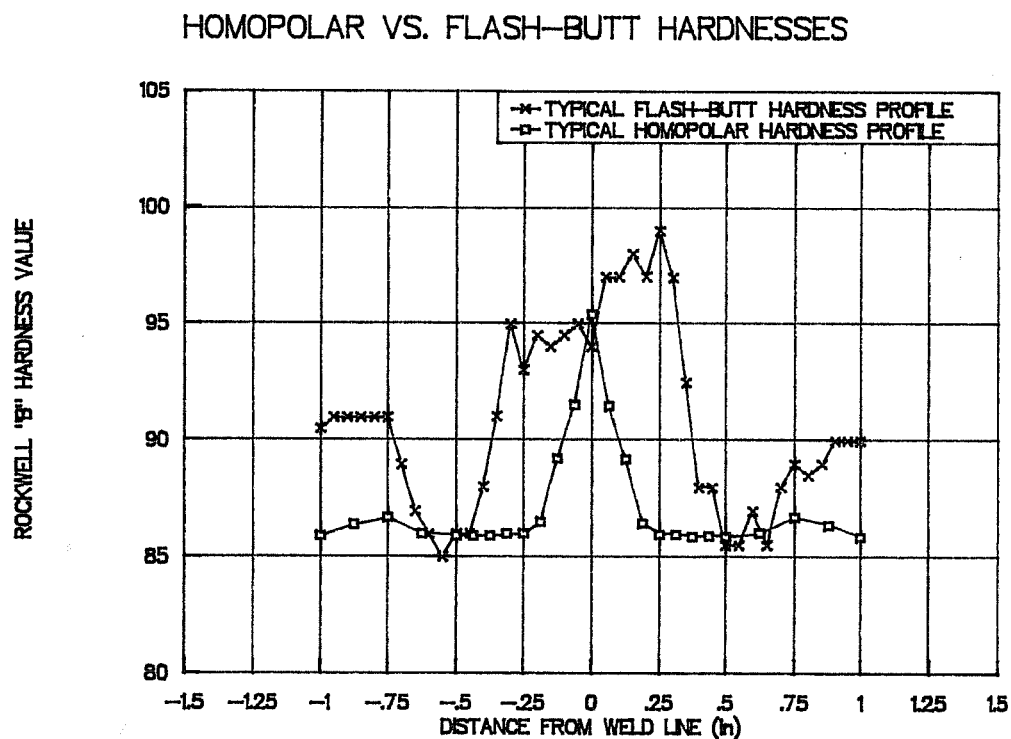


Figure 5.9 Homopolar vs. Flash-butt weld hardnesses.(7).

Figure 5.10 shows charpy v-notch test results for flash-butt welding and homopolar pulse welding. Both processes produced a severe reduction in weld line toughness. Research on flash-butt welding has shown that base metal toughness is regained through the application of post weld heat treatment.(7). The data for a normalized flash-butt weld is shown in figure 5.10.

HOMOPOLAR VS. FLASH-BUTT TOUGHNESSES

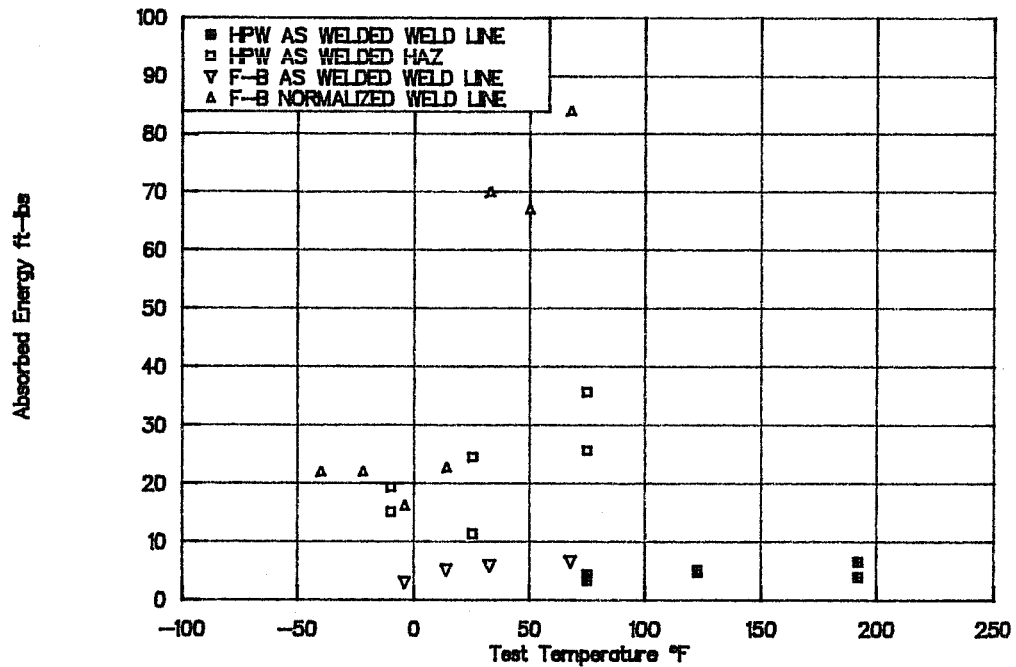


Figure 5.10 Homopolar vs. Flash-butt weld toughesses.(7).

As mentioned in chapter 4, normalized homopolar charpy specimens have not been tested. Testing of these is planned for the near future. Figure 5.10 also shows that heat affected zone toughesses remained high. Again, this should be attributed to grain refinement along the heat affected zone.

In conclusion, the homopolar thermal process seems to be gentler than the flash-butt thermal process. Because of this, lower peak hardnesses and higher quality heat affected zones are produced by homopolar pulse welding. This is point confirmed by the relative hardenabilities of the steels used in the investigations of homopolar and flash-butt welding.

5.1.3 FUSION WELDING THERMAL CYCLE.

Unlike homopolar welding and flash-butt welding, fusion welding relies on the melting of metal for the production of welds. The use of molten filler and base metals produces very complex metallurgical processes within the deposited weld metal and the heat affected zone. These changes are not experienced by resistance/forge welding systems since limited melting is produced by these processes. Fusion heat affected zones are subjected to severe thermal gradients. While weld metal is being deposited, the immediate area around the weld pool reaches temperatures well within the austenizing range. As the weld head moves away from the newly deposited weld pool, temperatures are quickly lowered through thermal conduction.

The heat affected zone constitutes an area of concern in fusion welding. High hardnesses and significant changes in toughness are not uncommon. Welding X65 line pipe using either SMAW or GMAW results in average maximum weld hardnesses of 104 Rb for GMAW and 98 Rb for SMAW.(2). Homopolar welding produced an average hardness peak level of 96 Rb while welding a higher carbon content steel.

Fusion welding is susceptible to the formation of residual stresses. As described above, the heat source of most fusion weld is limited to the arc and the weld pool. As the arc moves around the circumference of the pipe, residual stresses are produced by the non-homogeneous cross sectional thermal profile.

As long as the joint is not restrained axially, neither homopolar pulse welding nor flash-butt welding induce significant longitudinal residual stresses. Both heating and cooling are kept fairly uniform across these welds' cross section. Homopolar and flash-butt welding may, however, induce hoop residual stresses. These stresses are produced by faster cooling rates along the inner and outer wall surfaces.

Both homopolar and flash-butt welds have lower cast structure formation than fusion welds. Limited melting in resistance/forging processes eliminates the formation of cast structures.

5.2 COMPARISON OF WELD TURNOVER RATES.

Table 5.1 shows a comparison between flash-butt and common fusion welding production rates. All welds were made using 36" x 1" line pipe.

Table 5.1 Sample Weld Turn Over Rates.

WELDING PROCESS	PRODUCTION CYCLE TIME	JOINTS PER DAY
FBW	7 min	377
GMAW	12.5 min	211
SMAW	18 min	146

Table 5.1 Comparison of weld production rates.(7).

Homopolar welding is expected to have a 5 minute production cycle. Homopolar weld turnover rates are only limited by the time necessary to motor the homopolar generator and by time needed for proper pipe handling.

5.3 COMPARISON WITH INDUSTRIAL STANDARDS.

Before leaving this chapter it should also be noted that homopolar welding produced hardness levels that are acceptable under the DnV and BS codes. These standards set the strictest hardness requirements placed by any offshore pipeline construction code. DnV Rules 1981 limits maximum weld hardness to 260 Hv 5 kg for sour service conditions.(2). This converts to 103 Rb on the Rockwell "B" scale.

BS 4515-84 sets a similar limit.(2). Again, as welded homopolar welds showed an average maximum hardness of 96 Rb.

It was mentioned in chapter 4 that increases in hardness may occur as better interface heating is produced. It believed, however, that if higher hardnesses are incurred, these will remain comparable to flash-butt weld hardnesses, fusion weld hardnesses, and maximum allowable code hardnesses.

5.5 SIGNIFICANCE OF COMPARISONS.

Homopolar welding has shown its ability to produce welds whose quality is as good as either flash-butt or fusion weld quality. Added to this, homopolar welding has demonstrated very competitive production rates. Because of these characteristics, homopolar welding should be considered a strong contender for the laying of pipeline.

CHAPTER 6

CONCLUSIONS AND RECOMMENDATIONS

This thesis presented a discussion on preliminary results obtained during the investigation of homopolar pulsed welding for pipeline construction. Results have shown so far that homopolar welding is a viable alternative for pipe-laying applications.

6.1 KEY RESULTS.

A set of homopolar welds was fabricated and tested. Significant results were obtained through these welds. Base metal tensile strengths were developed by both reinforced and unreinforced specimens fabricated after the incorporation of the servo-controlled hydraulic system. Microstructural analysis, hardness testing, and toughness testing suggest the formation of high quality heat affected zones. In addition, reduction of the weld line hardnesses was achieved by normalizing the weldment. Additional testing is required to confirm that weld line toughness is regained through the application of post-weld heat treatment.

To prove its applicability, homopolar welds were then compared and contrasted to both flash-butt and fusion welds. The homopolar thermal cycle seems to be gentler than both the flash-butt and fusion thermal cycles. Because of this, homopolar welds are less susceptible to high hardness formation, toughness degradation, grain coarsening, and cast structure formation than either flash-butt or fusion welds.

6.2 QUESTIONS FOR CONTINUED RESEARCH.

It is clear that homopolar pulsed welding has a potential for industrial applications. Before it can be applied, several questions must be answered.

No clear reason has been formed to explain why some welds fabricated using the same apparent set of welding parameters show very different properties. Although improvements were made through the incorporation of a closed loop servo-controlled hydraulic system, other factors, such as lack of axial alignment, fixture

stiffness variation, and surface current variation, may be contributing to the presence of weld variability. Efforts to study this question are underway.

Parametric investigations have not been carried out due to the presence of weld variability. To date, most of the welds have been fabricated using weld parameters determined through past experience, or through trial and error. A more rational selection process is needed. Added to this, parametric studies are needed to form quality assurance flags. The use of these flags, coupled with the use of ultrasonic testing, may result in comprehensive non-destructive weld evaluations.

A clearer understanding of the interface heating process is needed. The presence of peripheral flaws along the inner pipe wall suggests that interface heating starts along the outer pipe wall, and gradually moves into the inner wall region. However, the physics behind this process are not well understood.

One factor affecting interface heating is initial surface resistance. The use of better controlled surfaces may result in higher and more homogeneous interface heating. This would then help ensure higher weld reproducibility. The use of controlled surfaces should not be considered a problem. Most pipe welding techniques already require some type of end preparation.

Improved interface heating may be achieved by studying the effects of upset loading rate. Using a ramp function for the application of upset load may result in higher, longer, and better controlled interface heating than using step functions. The present servo-controlled system allows the use of a ramped upset.

Temperature investigations need to be continued. Measurements have shown temperatures higher than what were initially anticipated.

Coupled with heating and temperature investigations, a complete characterization of heat treated weldments needs to be carried out. Unreinforced heat treated welds should be capable of developing base metal strengths. Testing of normalized charpy specimens is a priority. All toughness degradation must be eliminated through the application of post-weld heat treatment.

Finally, only 3.5" x 0.43" pipe has been welded. Different size pipes need to be welded to determine whether or not weld parameters can be scaled up or down easily.

To the credit of homopolar pulse welding, this investigation was done using a high carbon steel. Having welded this material is encouraging. The welding of lower carbon steels should be easier. Efforts are being planned to investigate this point.

REFERENCES

1. Walters, J.B., Aanstoos, T.A., "Welding and Billet Heating with Homopolar Generators." *Metal Progress*. April, 1985.
2. Teale, R.A., "OTC-5349 Deepwater Pipeline Specifications." *Proceedings for the 18th. Annual Offshore Technology Conference*. Houston, Tx. May 5-8, 1986.
3. Andersson, G.O., Weidemann, M., "OTC-4869 Flash Butt Welding for S-lay Barges." *Proceedings for the 17th. Annual Offshore Technology Conference*. Houston, Tx. May 6-9, 1985.
4. Stephens, P.R., Mandke, J., "OTC-4104 Probabilistic Analysis of Offshore Pipelines during Laying Operations." *Proceedings for the 13th. Annual Offshore Technology Conference*. Houston, Tx. May 4-7, 1981.
5. Gerwick B.C., "Installation of Steel Submarine Pipelines." *Construction of Offshore Structures*. John Wiley and Sons; New York, 1986.
6. Turner, D.L., "OTC-4870 Flash Butt Welding of Marine Pipelines Today and Tomorrow." *Proceedings for the 17th. Annual Offshore Technology Conference*. Houston, Tx. May 6-9, 1985.
7. Turner, D.L., "Flash Butt Welding of Large Diameter Oil and Gas Pipelines." *Pipeline Engineering Symposium*. 19th Annual Energy Conference and Exhibition. New Orleans, La. Feb 23-27, 1986. American Society of Mechanical Engineers.
8. Teale, R.A., Snoot, W.T., Trotter, J.J., "OTC-5532 Pulsed Spray Transfer for Automatic Pipeline Welding." *Proceedings for the 19th. Annual Offshore Technology Conference*. Houston, Tx. April 27-30, 1987.
9. Nicholas, E.D., Teale, R.A., "OTC-5813 Friction Welding Duplex Stainless Steel." *Proceedings for the 20th. Annual Offshore Technology Conference*. Houston, Tx. May 2-5, 1988.
10. Grant, G.B., Weldon, W.F., Rylander, H.G., Woodson, H.H., "Resistance Welding of Two Inch Schedule 40 Steel Pipe with a Homopolar Generator."

- Final Report, Astec Industries Research Project. Center for Electromechanics, The University of Texas at Austin. June 1978.
11. Gully, J.H., Aanstoos, T.A., Harville, M.W., "Homopolar Pulsed Welding for Offshore Applications." Paper submitted to the 9th International Conference on Offshore Mechanics and Arctic Engineering. Center for Electromechanics, The University of Texas at Austin. July 1989.
 12. Grant, G.B., Featherston, W.M., Keith, R.E., Weldon, W.F., Rylander, H.G., Woodson, H.H., "Homopolar Pulse Resistance Welding- A New Welding Process." *Welding Journal*. May 1979.
 13. Harville, M.W., "Surface/Pressure/Resistance Testing." Report on the effects of pipe end preparations on weld quality. Center for Electromechanics, The University of Texas at Austin. January, 1990.
 14. Boster, P., "Homopolar Pulse Welding Evaluation." Initial data report presented by Vetco Gray Inc. for the National Science Foundation Offshore Technology Research Center. October 1989.
 15. American Society for Metals, *ASM Metals Reference Book - A handbook of data about metals and metalworking*. p. 1.
 16. API Standard 1104-88, "Welding of Pipelines and Related Facilities." 1988.
 17. API Spec 5L: "Line Pipe." 1988.
 18. ASTM A370-77, "Standard Methods and Definitions for Mechanical Testing of Steel Products."
 19. Weldon, W.F., Aanstoos, T.A., "Homopolar Pulse Welding of High Strength Steel Line Pipe." Paper presented at the Advanced Pipe Fabrication Technologies Conference, New Orleans, La. April 18-19, 1988.

VITA

Francisco J. Noyola was born on June 26, 1966 in Mexico City, Mexico. He is the youngest of four sons born to Pedro and Martha Noyola. Francisco entered The University of Texas at Austin in 1984 after having completed high school at the American School Foundation in Mexico City. In 1988 he graduated with a Bachelor of Science in Civil Engineering with honors. During the Fall of 1988 he joined the graduate program in structural engineering at The University of Texas at Austin. In 1990 he completed the requirements needed to obtain a Master of Science in Structural Engineering. He now works as a designer of offshore structures.

Francisco is a member of Tau-Beta-Pi, Chi-Epsilon, the American Society of Civil Engineers, and the National Society of Professional Engineers.

Permanent Address:

Monte Athos 335A
Mexico D.F., Mexico 11000

This thesis was typed by Francisco J. Noyola.